

## Article

# An Equivalent Frame Digital Twin for the Seismic Monitoring of Historic Structures: A Case Study on the Consoli Palace in Gubbio, Italy

Daniele Sivori <sup>1,\*</sup>, Laura Ierimonti <sup>2</sup>, Ilaria Venanzi <sup>2</sup>, Filippo Ubertini <sup>2</sup> and Serena Cattari <sup>1</sup>

<sup>1</sup> Department of Civil, Chemical and Environmental Engineering (DICCA), University of Genoa, Via Montallegro 1, 16145 Genoa, Italy; serena.cattari@unige.it

<sup>2</sup> Department of Civil and Environmental Engineering (DICA), University of Perugia, Via G. Duranti 93, 06125 Perugia, Italy; laura.ierimonti@unipg.it (L.I.); ilaria.venanzi@unipg.it (I.V.); filippo.ubertini@unipg.it (F.U.)

\* Correspondence: daniele.sivori@unige.it

**Abstract:** Recent advances in computing performance and simulation tools allow today the development of high-fidelity computational models which accurately reproduce the structural behavior of existing structures. At the same time, advancements in sensing technology and data management enable engineers to remotely observe monitored structures in a continuous and comprehensive way. Merging the two approaches is a challenge recently addressed by the engineering research community, which led to the concept of digital twin (DT)—a simulation model continuously fed by sensor data which, throughout the whole lifespan of the structure, stands as its digital proxy. In the seismic field achieving such a task is still problematic, in particular for large and complex structures such as historical masonry palaces. To this aim, the paper proposes the integrated use of DTs and vibration data to support the seismic structural health monitoring of monumental palaces, discussing a practical application to the historical Consoli Palace in Gubbio, Italy. To overcome the computational limitations of classical approaches, an efficient equivalent frame (EF) model of the palace is built and continuously updated in quasi real-time based on modal information identified from vibration data. The performance and accuracy of the Equivalent Frame model are compared with those of a high-fidelity Finite Element representation, highlighting both their feasibility and limitations. Employing modal data recorded across the 15 May 2021 earthquake, the EF model demonstrates the ability to quickly assess the structural integrity of the palace in the post-earthquake scenario, as well as to forecast the residual capacity with respect to future seismic events.

**Keywords:** equivalent frame model; seismic structural health monitoring; model updating; structural damage; historical masonry buildings



**Citation:** Sivori, D.; Ierimonti, L.; Venanzi, I.; Ubertini, F.; Cattari, S. An Equivalent Frame Digital Twin for the Seismic Monitoring of Historic Structures: A Case Study on the Consoli Palace in Gubbio, Italy. *Buildings* **2023**, *13*, 1840. <https://doi.org/10.3390/buildings13071840>

Academic Editor: Humberto Varum

Received: 13 June 2023

Revised: 6 July 2023

Accepted: 16 July 2023

Published: 20 July 2023



**Copyright:** © 2023 by the authors. Licensee MDPI, Basel, Switzerland. This article is an open access article distributed under the terms and conditions of the Creative Commons Attribution (CC BY) license (<https://creativecommons.org/licenses/by/4.0/>).

## 1. Introduction

Recent advancements in digital computing, communication technologies, and measurement hardware are driving the digitalization of many engineering fields. The civil engineering sector is gradually adapting to this trend, with digital tools becoming a critical resource for supporting the decision making process in every phase of construction, from design to maintenance and future conservation of built assets.

A key step in this direction has been taken with the development of modern structural health monitoring (SHM) systems, in which different types of sensors are conveniently installed on the structure allowing to extrapolate parameters representative of the system's health in operating conditions, as well as those characterizing the environment and interacting with the system. Such parameters are identified and tracked in real time to detect abnormal states, i.e., states diverging from previous healthy structural conditions. Obtaining accurate and feasible information from monitoring structures, in other words extracting

engineering features from data, is a crucial task to support the structural maintenance and safety. In this regard, several techniques exist in the literature for identifying damage from vibration measurements of existing structures, mainly relying on modal parameters as damage-sensitive features [1]. Data-based approaches [2] are commonly used for early warning systems and damage detection, thanks to their efficiency and ease of implementation, and are today being fuelled by the advancement in machine learning [3]. However, these approaches typically rely on detecting statistically unusual responses with respect to those previously measured, lacking a strong relationship with the physical processes underlying the observed phenomena. This narrows the scope of applications to damage detection and localization, limiting the ability to provide insights about damage severity and predict future unobserved behaviors.

A more comprehensive damage identification framework is achieved by relying on a digital twin (DT) of the structure, a concept that civil engineering has recently inherited [4,5] from the industrial and mechanical fields and that is primarily embodied by the digitalization of the infrastructural management system, i.e., smart infrastructures [6] and smart buildings [7].

DT is a virtual simulation model that continuously acquires information from the physical reality of the structure, information which is encoded in the form of digital data coming from sensors. The model is able to enhance experimental data, providing a deeper understanding of unexpected behaviors or changes (due to aging, degradation, or structural damage) that may have occurred to the system. By incorporating sensors into the so-called “smart building” or “smart infrastructure” and developing a digital model, stakeholders such as concessionaires, managers, and decision makers can make informed decisions based on both data and models to guarantee the longevity and safety of their infrastructure [8]. Although the use of SHM for condition assessment, testing, and monitoring is becoming more and more prevalent, there is still a lack of agreement within the scientific community on its implementation. As a result, these practices are yet to be fully integrated into structural codes and standards, resulting in independent technological interpretations and implementations across different countries.

DTs are becoming essential for the preventive conservation of historical assets, combining building information modeling (BIM) [9] with SHM data and structural models [10,11]. As a cardinal principle of the DT concept [12], the need to continuously calibrate the model in quasi real time, thus solving an inverse optimization problem to minimize the difference between simulated and experimental response, can be exceptionally demanding from a computational viewpoint. This issue is widely testified in the literature, in particular dealing with the analysis of historical masonry structures. The complex architectural shapes arising from the search for beauty in the composition, the heterogeneous distribution of materials, the employment of different building techniques and structural systems, and the mark of historical interventions are all products of the long history of heritage structures, at the same time cultural value to be preserved and engineering challenge to be faced for this purpose.

On the one hand, these issues encourage the research community in integrating experimental data and mechanical models [13] towards the development of DT of historical masonry structures [14,15]. On the other hand, the computational burden of structural simulations is a limiting factor in employing physically based structural models as DT of historical buildings, particularly when dealing with almost real-time SHM.

In this context, the paper discusses the benefits and issues of integrating a structural DT to enhance the seismic structural health monitoring (S2HM, Ref. [16]) of historical masonry palaces, exploring its practical implementation for the dynamically monitored Consoli Palace of Gubbio located in Umbria Region, Central Italy. In particular, as a complementary approach to the commonly used finite element (FE) models, the research highlights the benefits of using a simplified equivalent frame (EF) formulation, which can be efficiently fused with continuous monitoring data using model updating techniques.

Section 2 proposes a general methodology to build and update a digital structural model for masonry palaces, suitable for pairing with a continuous monitoring system within the seismic SHM framework. Particular emphasis is given to the requirement of continuously updating the model with experimental modal data identified from the dynamic monitoring system, and how computational times play a key role in both the pre-earthquake calibration and post-earthquake simulation phases.

Section 3 presents the case study, the Consoli Palace of Gubbio, an ancient monumental masonry building continuously monitored with a mixed static–dynamic system by the University of Perugia. Focus is put on the behavior of the modal properties of the structure identified on a subdaily basis during May 2021, investigating any possible variations caused by a low-intensity earthquake that hit the structure on the 15th of the same month. The data-based analysis points out a slight but permanent reduction in natural frequencies of the structure as well as localized changes in mode shapes, revealing the potential occurrence of structural damage.

Section 4 exemplifies the methodology proposed to enhance the seismic monitoring of the palace, which employs a twinned structural model fuelled by monitoring data. In particular, the paper presents a detailed equivalent frame (EF) model of the structure, which is employed as a physics-based surrogate model. Its computational efficiency compared with the finite element (FE) counterpart allows for the continuous dynamic calibration of the elastic properties, which are directly updated based on daily-identified modal information. Employed a posteriori for the online assessment of seismic damage after the earthquake of 15 May 2021, the EF twin enriches the results of the data-based analysis, providing a model-based quantitative estimation of the reduction in the elastic stiffness of structural elements due to the damage caused by the seismic event.

Finally, in Section 4.3, the nonlinear capabilities of the EF twin are exploited to provide an effective offline tool to forecast the potential reduction in the seismic performance of the building after the earthquake. Based on experimental and numerical results from the literature, the constitutive laws of the masonry structural elements—in particular the parameters governing the secant stiffness and the resistance in the nonlinear phase—are degraded according to the updating of the elastic parameters. This allows for recovering, alongside the earthquake-induced reduction in stiffness identified from model updating, the unknown but complementary drop in masonry strength. The nonlinear static analyses performed on the updated/damaged model give an estimate of the reduction in global stiffness, resistance, and displacement capacity, information that can support the engineering judgement regarding the building safety and usability in the postseismic emergency phase.

## **2. Digital Twins for the Seismic Structural Health Monitoring of Masonry Palaces: Model-Driven and Data-Informed Methods**

### *2.1. General Framework*

Integrating a structural DT in common data-based methods for the condition assessment of structures provides a great extension to the capabilities of health monitoring systems, for both the condition assessment during operational conditions and damage evaluation after an extreme event, such as an earthquake [17]. In vibration-based SHM systems, the physical asset is sensed by a set of heterogeneous sensors that extract information about the response of the structure to operational or extreme actions, as well as from the environment. Through data analysis techniques, the feedback loop is closed by a real-time casting of the structural conditions, which can be entirely based on the acquired data. This implies that informed decisions are fully dependent, in this case, on the ability to extract meaningful engineering quantities from the acquired data. Among the other factors, this possibility depends (i) on the quality and amount of available data, which in turn reflects the sensitivity, extension, and denseness of the sensor network, and (ii) on the compliance with the hypothesis underlying the analysis technique, such as the classical requirement of white noise input to perform operational modal analysis. The most evident limitation, however, is the impossibility of making predictions for the long-term behavior

of the structure, in particular for conditions that differ from those measured (for example, the strong nonlinear and inelastic response during the earthquake as opposed to the linear elastic conditions of ambient vibrations).

Employing a physics-based structural DT allows for enriching the information inferred from data with the one provided by the physics of the model (Figure 1). These benefits, among others, include

- virtual sensing, i.e., the possibility to measure locations and phenomena that are difficult or impossible to measure with physical sensors;
- the estimation of uncertainties and model sensitivities;
- the identification of damage, intended as its detection, localization, and quantification;
- the forecasting of linear and nonlinear structural behavior, predicting the response for arbitrary loading and environmental conditions.

Informed decisions are thus driven by the model response, which, in turn, is informed by experimental data. This scheme allows for casting the condition of the structure almost in real time. Moreover, based on the model's computational efficiency, such integration allows for quasi-real-time (online) simulations or, more often, for deferred-time (offline) forecasting of the structural behavior in future unmeasured states. Indeed, this general framework is still heavily case dependent and lacks a general systematic implementation for civil structures.

The following paragraphs discuss different strategies to achieve a model-driven and data-informed seismic health assessment of dynamically monitored masonry palaces, focusing first on the suitable structural modeling approaches (Section 2.2) and, second, on possible data fusion techniques (Section 2.3).

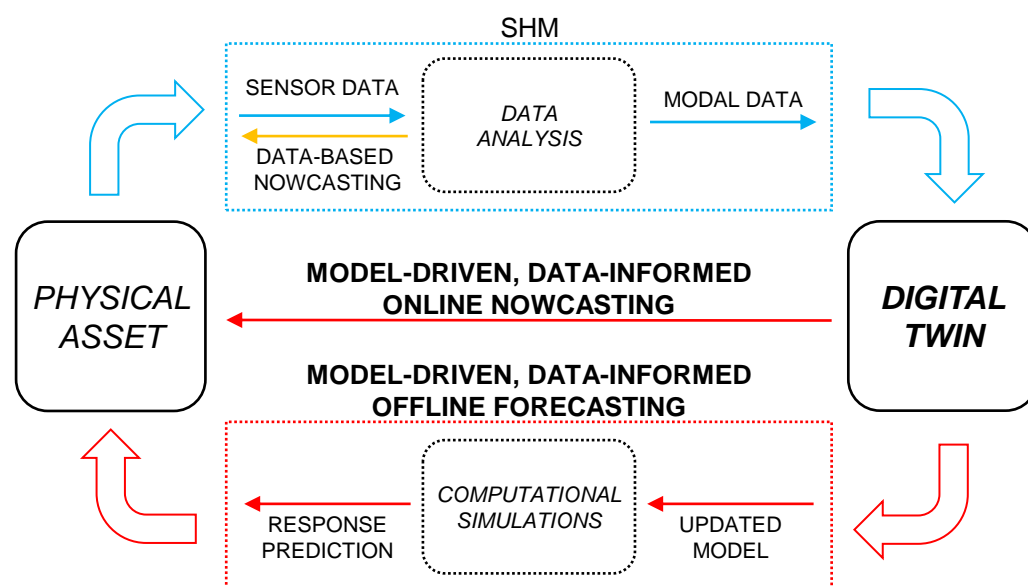


**Figure 1.** Conceptual diagram of the SHM-DT framework for the condition assessment of physical assets.

## 2.2. Structural Modeling

The conservation and seismic protection of monumental masonry buildings pose significant challenges for the engineering community due to their intrinsic vulnerability to earthquake actions and intricate structural behavior. Heritage buildings are typically large structures that have undergone spontaneous transformations in the past, resulting in a current structural configuration characterized by geometrical irregularities, material heterogeneities, and peculiar structural systems. As a result, assessing the health and safety conditions of these structures presents some critical issues to be solved to achieve a reliable structural analysis.

One of the main challenges is the choice of the modeling strategy. Among the possibilities, deeply reviewed in [18,19] and discussed from a seismic engineering viewpoint in [20,21], finite element (FE) models constitute the most common choice for monumental assets. According to the classification proposed in [20], which refers to the modeling and discretization scales, these models may be classified as CCLM (continuous constitutive law models) in which the behavior of the masonry material is described by homogenized constitutive laws of phenomenological or micromechanical derivation. The literature is rich in examples of FE models built and employed to analyze the structural behavior of historical masonry structures, such as towers [22], churches and monasteries [23–25], fortresses and castles [26,27], and, not least, palaces [28–30].

The FE approach provides a very detailed representation of the structure, which comes at the cost of (i) a large initial effort devoted to the modeling phase (even though, today, automatized modeling strategies based on laser-scanned point clouds are becoming a real possibility [15,31,32]); (ii) dealing with a variety of input parameters to define the material and mechanical behavior in the linear and nonlinear regimes, especially in the calibration phase; and (iii) a significant computational demand in the simulation phase, depending on the complexity of the model and on the phenomena investigated. The second and third points can introduce limitations for the aspired SHM–DT integration in both the model updating and forecasting phases, particularly when dealing with earthquake actions—which imply strong nonlinearities and long computational times.

Focusing on the analysis of the response to seismic actions, in the case of historical masonry palaces, a complementary modeling strategy is provided by the equivalent frame (EF) formulation [33]. This approach falls within the class of SEM (structural elements models), in which macroscopic structural elements governed by a limited number of mechanical parameters discretize the masonry continuum. In the equivalent frame representation, only specific areas of masonry walls are explicitly modeled, the vertical and horizontal portions of masonry between openings exhibiting structural damage due to earthquake actions (namely, piers and spandrels). Deformability is thus narrowed to these elements, whereas the remaining parts of the walls are assumed to behave rigidly (rigid nodes). The three-dimensional model results from the assemblage of vertical frames, which commonly accounts for the sole in-plane stiffness of masonry panels, with horizontal diaphragms of finite stiffness representing the flooring system. An in-depth discussion regarding the EF implementation, which includes algorithms, failure criteria, static and dynamic analysis techniques, is reported in [33].

This approach shares some similarities with classical model reduction techniques, which aim at lowering the computational complexity of mathematical models by reducing their dimension, i.e., their degrees of freedom, accepting an approximation error with respect to the original model. The EF concept intrinsically follows this route, since the discretization condenses all the degrees of freedom of the structure at the scale of structural elements. This strategy strongly reduces the model's complexity and improves its performance, with the main limitations of losing (i) the resolution to describe scales smaller than that of masonry panels—such as the material continuum—and (ii) the possibility to capture unexpected (unmodeled) deformations happening in the rigid parts.

The morphological peculiarities that palaces typically share with ordinary masonry buildings, above all the regularity in the layout of the openings in the facades, suggest the EF modeling approach to be a suitable analysis tool. Indeed, other assumptions of this formulation have to be judged with expert knowledge on a case-by-case basis. A common example is the hypothesis of in-plane behavior of masonry walls, which is satisfied in the case of stiff horizontal diaphragms and by the presence of adequate wall-to-wall and wall-to-diaphragm connections. Due to the complexity and heterogeneity characterizing existing masonry buildings, there are several proposals in the literature to calibrate, adapt, or improve the rules governing the equivalent-frame representation to deal with common issues encountered in the modeling of these structures. Among the others, these issues are posed by an irregular arrangement of the openings [34–36], the presence of deformable

diaphragms [37,38], vaulted floors [39,40] and arch systems [41,42], the quality of the connection between orthogonal walls [43]. Undoubtedly, the relevance of these factors in the simulation of the global behavior of the structure and local behavior of its subsystems can be accurately evaluated from the comparison with experimental measurements [44–46] or with the results of a more detailed FE model, often adopted in the literature as a benchmark reference [47–51].

Following the guidelines provided by the literature, the EF technique can be reliably employed for the structural modeling of masonry palaces. Structural element modeling, even though simplified from the mechanical viewpoint, is still accurately representative of the building's seismic behavior and comes with the main advantage of being extremely computationally efficient when compared with higher-fidelity FE models. In the DT framework, the limited number of elements and degrees of freedom allows the updating phase to be solved in seconds (see the following Section 2.3), whereas prediction of nonlinear behavior can be obtained in a reasonable time ranging from several minutes to a few hours, even for large and complex structures—thanks to the efficient constitutive laws defined at the scale of structural elements.

### *2.3. Continuous Model Updating for Model Calibration and Real-Time Damage Assessment*

In structural engineering, model updating is the process of calibrating a structural model to improve its accuracy in reproducing the actual behavior of the structure subjected to different types of loading [52]. In the framework of a continuous vibration-based SHM, the structure is monitored during its operational conditions. Model updating involves, in this case, a periodic comparison—which can take place daily, hourly, or practically in real time, based on the characteristics of the acquisition and the computational effort required—between the modal parameters predicted by the model (natural frequencies and mode shapes) and the ones identified from ambient vibrations, i.e., from the low-amplitude oscillations generated by an ideal frequency-flat spectral input provided by environmental loading. In this case, among the several parameters involved in the direct eigenvalue problem, the sensitive ones (whose small change significantly influences the modal behavior [53]) can be tuned using an optimization algorithm, with the aim of minimizing the differences between the predicted and measured dynamical responses. These statements still hold true when dealing with the condition assessment of the structure after an extreme event, such as an earthquake, which is typically carried out by comparing the operational states before and after the loading to detect damage [54].

Model updating can be thus formulated as an inverse optimization problem. To approach it, two categories of optimization techniques can be employed: global and local optimization [55]. Global optimization algorithms, either deterministic, stochastic, or heuristic, try to explore the entire search space in order to find the global minimum of the objective function, the function that measures the difference between the predicted and target response. The objective function typically combines, through a tradeoff, the discrepancies between simulated and identified natural frequencies and mode shapes. These algorithms are generally more computationally expensive and thus slower, but are more likely to find the optimal solution, even if the solution space is nonlinear or nonconvex.

In contrast, local optimization algorithms focus on finding the minimum of the objective function within a small region of the space neighboring a known solution. These iterative algorithms are typically faster and more efficient but, at the same time, are more likely to become stuck in a local minimum, which may not be the optimal one.

The choice between global and local optimization techniques for model updating depends on the careful consideration of the complexity of the model, the specific issues to be addressed, and the available computational resources. A combination of both global and local optimization techniques may be used in some cases to achieve a balance between accuracy and efficiency. The ability to thoroughly explore the parameter space makes global optimization algorithms ideal for the first model calibration, a phase potentially dominated by several unknowns and large uncertainties (for example, related to the mechanical

properties of the building materials) but in which computational time is not a primary issue. Local optimization algorithms, instead, fit better the requirements of the continuous model updating, where the starting solution is already known from the first or previous calibrations, and relatively small changes are expected in the target solution (such as those due to changes in environmental conditions, to aging or degradation, to structural damage). Finally, low computational times are mandatory to keep track of real-time data coming from the monitoring system.

Overall, the large number of simulations involved in the model updating phase can become the limiting factor in employing physically based DT for the condition assessment of historical buildings. The calibration of a high-fidelity finite element (FE) model can be reasonably pursued when dealing with simple beamlike structures, such as towers [56–60], in these cases even in quasi real time [61–64]. Depending on the structural complexity and the level of detail of the model, even with modern computing capabilities, this task can become unfeasible due to unsustainable computational times.

One way of alleviating this burden is constructing approximation models, or surrogate models, as closely as possible representative of the original simulation model while being computationally cheaper to evaluate. Surrogate models are black box mathematical representations of a system. These models are typically built using a limited number of simulations and can be used to rapidly predict the behavior of the system under different conditions. The use of surrogate models has several advantages over traditional simulation methods. On the one hand, surrogate models can greatly reduce the computational cost of simulations, while, on the other hand, such models inherently incorporate some degree of uncertainty (due to the limited number of simulations they are based on). There are several types of surrogate models that can be used for structural applications. One popular type is the polynomial chaos expansion, which uses orthogonal polynomials to represent the system's behavior [65]. Another type is the Kriging model [66,67], which uses Gaussian processes to interpolate between the simulated data points. Despite their many advantages, surrogate models do have some limitations. Surrogates may not accurately capture the behavior of the system under new operating conditions. Additionally, the accuracy of the model may degrade over time as the system evolves or as new data become available. Moreover, they may not be appropriate for all types of systems, particularly those with highly nonlinear behavior.

For the seismic monitoring of masonry buildings and palaces, as previously discussed in Section 2.2, a possible alternative approach is to rely on an equivalent frame (EF) representation of the structure. This model can be considered for all purposes a physics-enhanced surrogate, an efficient model that is capable of simulating the global seismic response of the structure based on the underlying mechanics of a limited number of macroelements, the masonry panels. The reliability of this simplified approach in simulating the seismic response of masonry buildings, even in the strongly nonlinear regime, is well documented in the literature. Previous validations include, among the others, the comparison with the results of shaking table tests [68–70], with high-fidelity micro modelling techniques [35], with acceleration measurements acquired on monitored buildings recently hit by earthquakes [44–46,71]. The employment of the EF model in the framework of seismic monitoring is still evolving from an exploratory stage, which nonetheless is following recent satisfactory outcomes obtained from the simulation of the modal dynamic behaviour of existing buildings (see [38,44]) as well as some validations for low-amplitude vibrations [72] and in the weakly nonlinear regime [73].

The EF discretization allows for greatly reducing the complexity of the simulation and, as a consequence, reducing the computational effort paying the cost of spatial resolution (which is limited by the scale of structural elements). As it will be shown in the applications (Section 4), this efficient model can be employed directly in continuous updating procedures, making it effectively a structural DT of the monitored structure—enriching the information extracted from the monitoring system in the immediate aftermath of the earthquake,

evolving data-based damage detection to a more robust model-driven and data-informed damage assessment, which can include also damage localization and quantification.

#### *2.4. Model-Driven Data-Informed Forecasting of the Postseismic Structural Behavior*

As discussed in the previous paragraph (Section 2.3), ideal DT models should have capabilities that can be readily employed online in parallel to data acquisition, i.e., in a quasi-real-time framework, to support the structural health monitoring and the condition assessment of monitored buildings after the earthquake, enriching the information provided by vibration data alone. These tasks commonly involve, among others, an initial evaluation of potential damage to the structure, which is usually followed by a more detailed evaluation of the residual structural capacity.

The first task (ideally including all three levels of damage assessment, detection, localization, and quantification) can be achieved through model updating and provides useful information related to the actual damage diffusion and gravity in the real structure, as well as quantitative estimates of the degradation of the mechanical properties of the structural elements.

More accurate evaluations regarding, for example, the structural functionality, are usually carried out offline since they require computationally expensive nonlinear simulations. These analyses are commonly addressed to verify the operativity of the structure (in particular, if the structure holds a strategic function in the management of the seismic emergency of the urban area, as often happens to town hall buildings in Italian municipalities), its usability and safety (to allow the following in situ inspections, the recovering of artistic assets in safety conditions, eventually the return of occupants), and finally, the residual capacity to future seismic actions to ensure the protection of human lives in the case of aftershocks.

In this respect, FE modal surrogates are well suited for quick damage assessment (Section 2.3) but lack the capabilities to forecast the behavior of the structure after the earthquake. EF models, on the other hand, have roughly the same efficiency in the elastic regime and are able, in a few tens of minutes, to simulate the nonlinear response of the structure to known or expected seismic actions. Thus, they can be used to accurately simulate structural damage and the subsequent loss of capacity, making them a valuable tool to assess the response to future shocks.

Simulations regarding the general seismic behavior of the structure can be carried out in advance, by selecting plausible seismic input and simulating and interpreting the expected structural response in a statistical sense. When effectively synthesized, these results become immediately useful once the earthquake strikes. For example, the recently proposed behavioral charts that relate a measured frequency reduction to the expected global damage level reached by the structure [74] allow for a quick model-driven, data-informed evaluation of the damage level expected on the structure. Indeed, a precise evaluation of the effects caused by a specific earthquake that hit the structure can be only carried out only after the event. The seismic input measured at the base or in the proximity of the building is employed directly, when available, to accurately simulate the nonlinear structural response to the earthquake and, in the case of a monitored structure, to compare it with response measurements [45].

Following the methodology outlined, the following paragraphs present the development of an EF digital twin for the historical Consoli Palace of Gubbio, Italy. The DT is employed to support the evaluations of structural integrity after the seismic sequence that hit the building on 15 May 2021, tackling the online damage assessment based on continuous model updating (Section 4.2) and the offline evaluation of the building residual capacity based on nonlinear static analyses (Section 4.3).

### 3. The Consoli Palace of Gubbio, Italy, and the Seismic Sequence of 15 May 2021

#### 3.1. The Palace: Dynamic Monitoring System and AVT

The Consoli Palace, situated in Gubbio, Umbria (Central Italy), is an impressive architectural complex constructed during the 14th century. It stands out as one of the most daring constructions of its time, towering over the town's main square at a height of 60 meters. The palace comprises a central body, a panoramic loggia, and a bell tower, accessible from the rooftop. The load-bearing walls of the Consoli Palace have a thickness of about 1.2 m, measured from in situ inspections, and each floor is characterized by differently oriented and distributed vaulted ceilings. The building is constructed with a homogeneous texture of calcareous stone masonry. The east- and west-side facades of the palace are adorned with round-arched windows and merlons on the rooftop.

As per the seismic regulations outlined in the Italian technical standard NTC2018 [75], the site is characterized by a peak ground acceleration (PGA) of 0.227 g with a 10% probability of exceedance in a 50-year time frame (return period of 475 years). In addition, the city is situated near the Gubbio normal fault, a preorogenic fault that stretches for 22 km [76]. To monitor the high seismicity of the area, a dense network of seismic stations, known as Alto Tiberina Near Fault Observatory—TABOO, was established in 2014 [77].

In 2017, a continuous monitoring system was installed in the palace, which underwent further improvements in July 2020 by increasing the number of sensors (A1–A12 with reference to Figure 2). The Department of Civil and Environmental Engineering at the University of Perugia designed and managed the system within the framework of European and national projects. The acquisition system consists of several components:

- a mixed data acquisition system wired to sensors (NI CompactDAQ-9132 model equipped with NI 9234 acquisition modules for accelerometers with 24-bit resolution, 102-dB dynamic range, and anti-aliasing filters);
- a NI 9219 acquisition module with 24-bit resolution,  $\pm 60$  V range, 100 S/s for LVDTs and thermocouples);
- a wireless network (LoRaWAN system technology).

The monitoring system comprises twelve unidirectional accelerometers named A1–A12, located and oriented as schematically reported in Figure 2. The accelerometers, model PCB393B12, have the following characteristics: a measurement range of  $\pm 0.5$  g, a frequency range of 0.15–1000 Hz, a broadband resolution of 8  $\mu$ g, and a resonant frequency  $\geq 10$  kHz. Additionally, four linear variable transducers (model S-series) with a measurement range of 0–0.5 mm and a resolution of 0.31 m (D1–D4), and six thermocouples (T1–T6, model K-type) are included in the system.

Acceleration data are recorded in files that span a duration of 30 min of measurements with a sampling frequency of 100 Hz, then downsampled to 40 Hz. Measurements of crack amplitudes and temperature values are acquired every half hour. All the data are consistently saved in a cloud-based storage system, conveniently accessible via a web-based platform. The data are constantly post-processed by means of the MOVA integrated software, an automated tool based on the covariance-based stochastic subspace identification (SSI) technique. Environmental effects are removed from original signals through the multiple linear regression (MLR) statistical models after analyzing the time series of ambient and material temperature measurements during the training period of one year. More details on the analyzed case study can be found in [67,78,79].

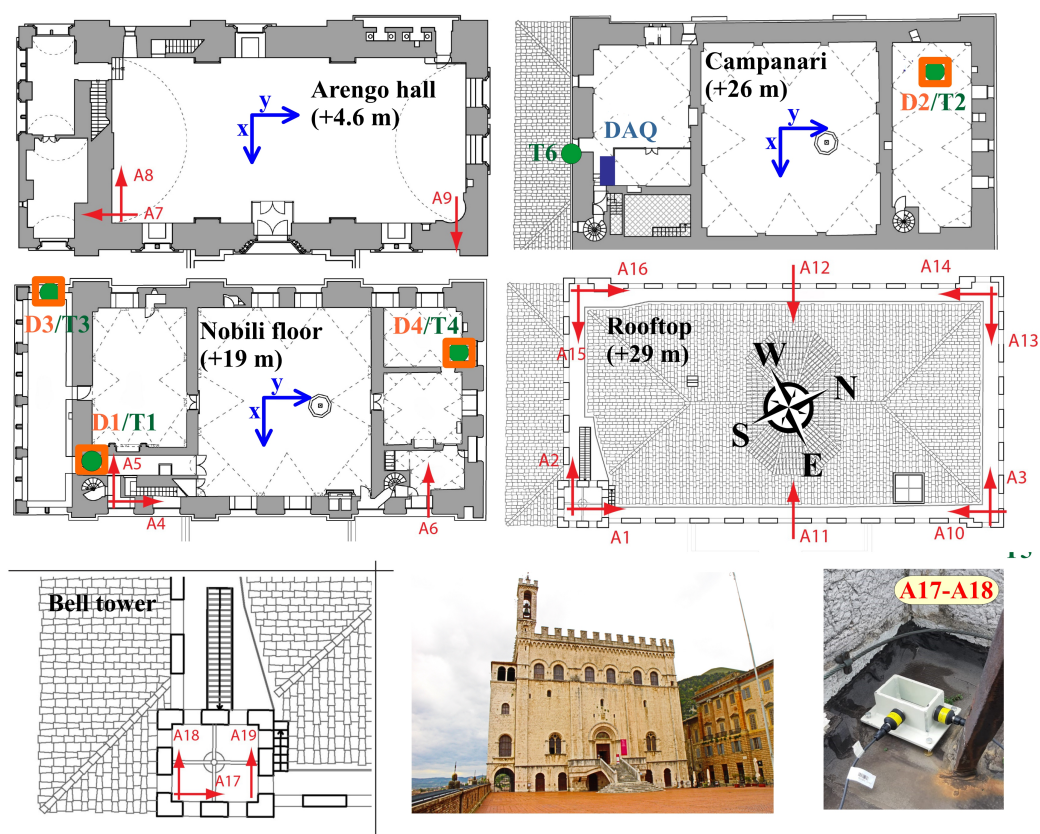


**Figure 2.** A schematic representation of the SHM system of the palace (A1–A12) and of the AVT extended sensors network (A1–A19).

For the purpose of tackling the initial calibration of computational models, an AVT was performed on 7 May 2021 by including channels A13–19 (Figure 2). More in detail, channels A13–A16 allowed for improving the definition of the rooftop’s dynamic behavior, whereas channels A17–A19, placed at the top of the bell tower, were included to assess the impact of this slender element on the global dynamics of the palace. The identification results are presented here as a reference for the following discussion. The first five identified modes (Table 1) are found in the frequency range 2.3–4.2 Hz, corresponding to the range of periods 0.24–0.43 s. The labels “G” and “L” indicate, respectively, a global and local mode, with a dominant “F” flexural or “T” torsional component developing along the  $x$ ,  $y$ , or  $z$  reference axes (see Figure 2).

**Table 1.** Natural frequency  $f$  and damping ratio  $\zeta$  identified for the first five natural modes of the palace during the AVT performed on 7 May 2021.

Mode	Type	$f$ (Hz)	$\zeta$ (%)
1	G-F <sub>x</sub>	2.296	1.121
2	L-F <sub>y</sub>	2.989	0.751
3	L-F <sub>x</sub>	3.508	0.779
4	G-F <sub>y</sub>	3.743	2.477
5	G-T <sub>z</sub>	4.172	1.104

### 3.2. Continuous Monitoring across the Seismic Sequence of 15 May 2021

On 15 May 2021, a minor seismic sequence took place with the epicenter in Gubbio, Italy, characterized by the strongest shock of magnitude  $M_w$  3.9 hitting at 07:56:01 UTC, and other slight shocks occurred in the following days, with a maximum magnitude up to  $M_w$  3.1. Ground accelerations have been recorded by the measurement station “Gubbio Parcheggio Santa Lucia” (GBSL) of the Italian Strong Motion Network (RAN, [80]), a dense

network of seismic stations distributed all over the Italian territory managed by the Italian Department of Civil Protection. The station is lying at a distance of around 700 m from the epicenter (Figure 3a) on a soil of class B according to Eurocode 8 ( $V_{S,30} = 765 \text{ m/s}^2$ , quite close to the  $800 \text{ m/s}^2$  threshold of class A representing the bedrock condition). The waveforms downloaded from the ITACA database [81] show that the peak ground accelerations (PGA) reached  $102.38$ ,  $77.83$ , and  $47.15 \text{ cm/s}^2$  along the HNE, HNN, and HNZ components, respectively (Figure 3b, top). The response spectra show that the energy content of the horizontal components is localized in the range  $0.1\text{--}0.25 \text{ s}$  (Figure 3b).

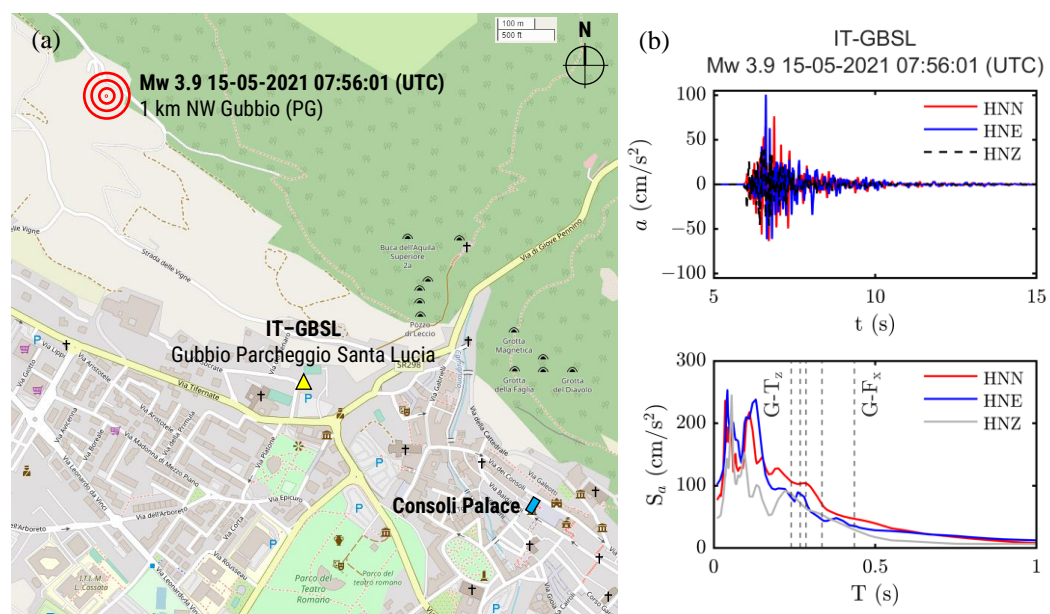


**Figure 3.** Earthquake of 15 May 2021 in Gubbio, Italy. (a) Location of the epicenter, of the RAN seismic station GBSL and of the Consoli Palace. (b) Accelerations measured by the GBSL station along the HNN, HNE, and HNZ components, and corresponding response spectra (damping 5%).

Because of an electrical interruption affecting the SHM system until around 08:00 UTC, continuous vibration data acquired on the palace are available only before and after the event [82]; nonetheless, they remain extremely valuable for the purposes of this work. To test the reliability of a continuous updating of the structural models of the palace (see Section 4.1) and their ability to support the post-earthquake damage assessment, a month of modal data going from 1 May to 31 May and including the earthquake event is first analyzed and, later in the paper, employed as baseline data set to carry out the model updating and the following damage assessment.

To contain their variability, the natural frequencies and mode shapes of the first five modes of vibrations—which have been identified from the research unit of Perugia from continuous 30 min long acquisitions and depurated from environmental effects—have been averaged over each day. Further information regarding the continuous dynamic identification is provided in [82].

The Consoli Palace, located at a distance of around 1.25 km from the epicenter of the main earthquake, exhibited a mild evolution of the pre-existing damage mechanisms, which are related to some observed cracks affecting the north facade and its connection with the orthogonal west facade. An in-depth assessment of the damage caused by the seismic sequence, endorsed by the fusion of in situ inspections with FE-based computational simulations, is reported in [67]. For the purpose of the following applications, it should be highlighted that, as a consequence of the low intensity of the shock, the mild severity of the damage pattern does not pose a relevant threat to the structural integrity of the palace.

Nonetheless, as reported in [67], a permanent frequency decay has been observed for the first five modes of vibration, ranging from 1.1% to 1.4% for the global modes of the palace, from 2.3% up to 2.7% for the local modes of the bell tower.

This change is already evident by looking at the average daily value of the natural frequencies (referred to as  $\hat{f}$  in the following) in the short observing period of the month of May 2021 (Figure 4a). The relative frequency variations with respect to the initial observation  $\Delta\hat{f}/\hat{f} = -(\hat{f} - \hat{f}_0)/\hat{f}_0$  (Figure 4b) show permanent reductions in the range 2–4%, whereas those related to the previous day (subscript  $d - 1$ , Figure 4d) clearly highlight how those reductions are maximum across the day of the main shock. Variations in mode shapes, which are estimated by the modal assurance criterion (MAC) indicator [83], seem to be generally contained (MAC values higher than 0.94, Figure 4c,e). More in detail, the daily natural frequencies across 15 May, their relative reductions, and cross-MAC are reported in Table 2.

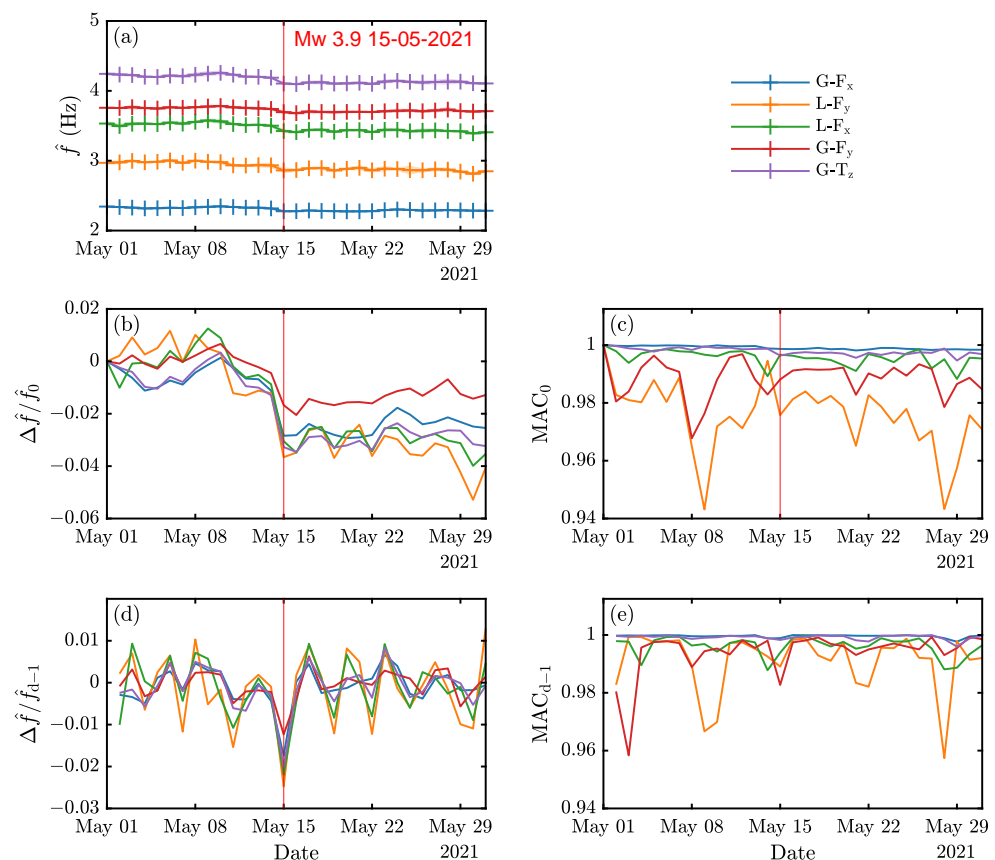


**Figure 4.** First five identified modes of vibrations and their observed variations in May 2021, highlighting the effects of the Mw 3.9 seismic shock of 15 May. (a) Daily-averaged frequency  $\hat{f}$ , (b,d) relative variations with respect to the first observation  $\hat{f}_0$  and previous-day observation  $\hat{f}_{d-1}$ , (c,e) MAC values.

For what concerns the long-term behavior, analyzing the average variations—related to the average frequencies  $\bar{f}$  and average mode shapes  $\bar{\Phi}$  of the pre- and post-event observation periods—confirms the occurrence of permanent changes in mode frequencies, in particular those related to the local modes of the bell tower (right side of Table 2). In general, these changes appear much more limited for mode shapes. Indeed, the average indicator  $\overline{\text{MAC}}$  does not suggest a certain mode among those identified to be the most affected by seismic damage.

**Table 2.** Change in natural frequencies caused by the earthquake of 15 May 2021, both with respect to daily-averaged values ( $\hat{f}_{14-05-21}$ ,  $\hat{f}_{15-05-21}$ , and relative variations  $\Delta\hat{f}/\hat{f}$ ) and long averages over the whole pre- and post-earthquake observation periods ( $\bar{f}_{pre}$ ,  $\bar{f}_{post}$ , and relative variations  $\Delta\bar{f}/\bar{f}$ ).

Mode	Type	$\hat{f}_{14-05-21}$	$\hat{f}_{15-05-21}$	$\Delta\hat{f}/\hat{f}$	MAC	$\bar{f}_{pre}$	$\bar{f}_{post}$	$\Delta\bar{f}/\bar{f}$	$\bar{MAC}$
1	G-F <sub>x</sub>	2.317	2.277	−0.0174	0.9991	2.330	2.285	−0.0194	0.9993
2	L-F <sub>y</sub>	2.934	2.861	−0.0247	0.9890	2.970	2.869	−0.0340	0.9990
3	L-F <sub>x</sub>	3.501	3.424	−0.0220	0.9931	3.531	3.425	−0.0299	0.9974
4	G-F <sub>y</sub>	3.741	3.695	−0.0123	0.9766	3.760	3.705	−0.0144	0.9928
5	G-T <sub>z</sub>	4.188	4.104	−0.0200	0.9982	4.220	4.117	−0.0244	0.9984

To achieve a preliminary data-based localization of the occurred damage, a more accurate analysis has been carried out on the whole set of considered modes by estimating different coordinate-based damage indicators, the coordinate MAC (COMAC) in its original [84], scaled (“-s”) [85] and enhanced (“-e”) [86] versions, as well as the variational MAC (“-var”) [87]. The COMAC indicator, intended as the difference from unitary value, is expected to be higher for the coordinate that underwent the most abrupt changes. The variational MAC highlights the coordinates to be subsequently removed from the MAC calculation to maximize its average increase over all modes.

The standard and scaled COMAC indicators evaluated between the mode shapes identified the day of the earthquake and those of the previous day (Figure 5a) suggest sensors A6 and A11, both directed along x (the direction parallel to the short sides of the palace), to be the most affected by earthquake effects. Sensor A6 is located at the Nobili floor close to the northeast corner, whereas sensor A11 is on the rooftop, at the middle of the main facade. The enhanced COMAC points out sensor A2, located on the rooftop and close to the south side, as the most affected sensor, followed in turn by A6 and A11. This result is in better agreement with the MAC-var analysis (Figure 5b). The removal of channel A2, in fact, provides the maximum gain in the average value of the MAC, improving mostly the correlation of the global mode G-F<sub>y</sub>. This mode develops in the orthogonal direction y (parallel to the long sides of the palace) but includes some torsional effect, which can explain such an outcome.

The same indicators estimated on the averaged mode shapes of the pre- and post-event observation periods seem to be more coherent among themselves. All the COMAC indicators (Figure 5c) agree with the MAC-var analysis (Figure 5d) in identifying locations A2 as the most affected by the long-term effects of the earthquake. The removal of this sensor from the MAC analysis is optimal in an average sense and again is improving mostly the correlation of the global mode G-F<sub>y</sub> along the orthogonal direction.

Data-driven results point out, in general, the x direction as the most affected by seismic damage, damage that can be roughly localized—but hardly quantified—in the south perimeter walls of the palace (in accordance with the evolution of the pre-existing crack pattern observed during the in situ inspections, see [67]). These outcomes will be taken as reference in the applications of the proposed model-based data-informed procedures of the following sections.

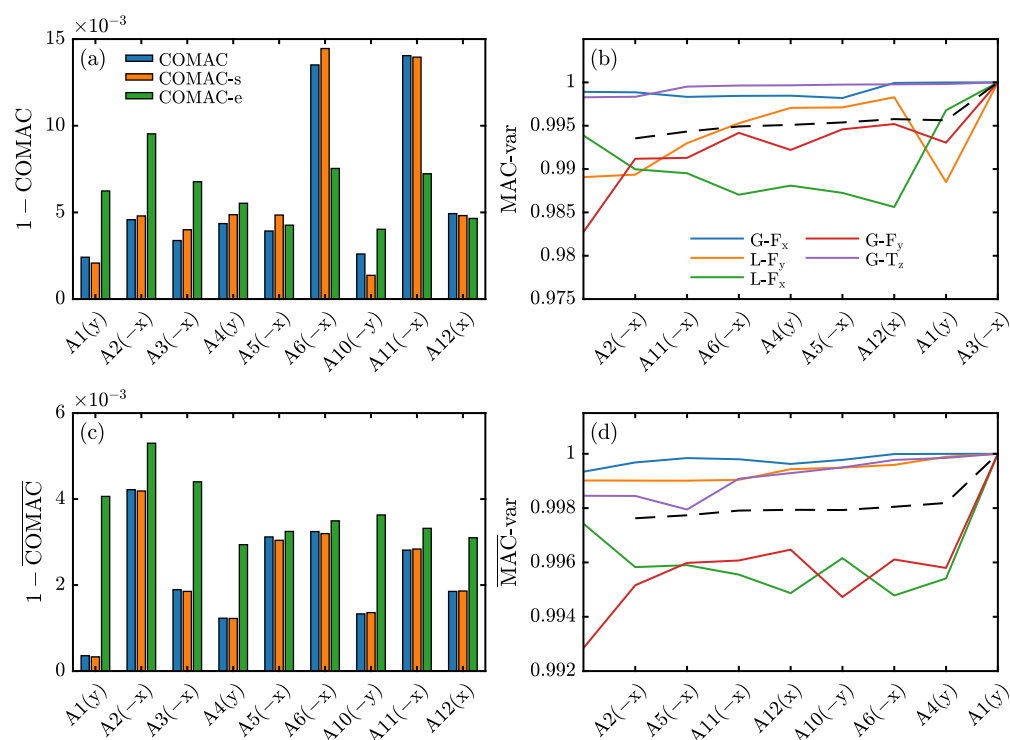


**Figure 5.** COMAC and MAC-var indicators estimated after the earthquake of 15 May 2021, (a,b) with respect to the previous day, (c,d) to long averages over the whole pre- and post-earthquake observation periods.

#### 4. Continuous Updating of DTs: Applications

##### 4.1. Equivalent Frame (EF) and Finite Element (FE) Models of the Palace

To deepen the analysis regarding the seismic behavior of the palace, keeping in mind the aim of developing a structural DT to support the postseismic evaluations (Section 2), the structure has been modeled according to two different approaches (among those discussed in Section 2.2), the equivalent frame (EF) and finite element (FE) formulations.

The EF model of the structure (Figure 6a) has been built by the research unit of the University of Genoa in the framework of the PRIN research project DETECT-AGING (Degradation Effects on sStructural safety of Cultural heriTAGE constructions through simulation and health monitorING).

The three-dimensional model has been meshed and assembled employing the commercial software 3Muri (S.T.A. DATA, version 13.9.0.0), whose solver (TREMURI in the following) has been developed at the University of Genoa [33]. Based on the building geometry and openings arrangement and according to the rules commonly employed for ordinary masonry buildings, each masonry wall is automatically subdivided into deformable piers and spandrels, which are connected by rigid nodes. Finally, the three-dimensional model of the structure is built assembling vertical walls and horizontal diaphragms. Manual tweaking of the original mesh has been carried out to improve the EF discretization of the external walls of the Arengo Hall (Section 3.1). This area is characterized, in fact, by a relevant interstorey height—close to 15 m—and relatively small openings. The alteration of the original mesh made the height of the piers more representative of the expected deformable portion of the walls, reducing at the same time the excessive dimensions of rigid nodes, which may otherwise produce an overestimation of the overall stiffness. The development of the model, the optimization of the mesh, and the first dynamic calibration of the model based on the extended AVT campaign of May 2021 (Section 3.1) are described in detail in [88]. The EF model here presented has been recalibrated according to the new updating scheme presented in Section 4.2, which considers just four predefined regions and four updating variables, namely, the regions' Young moduli.

The three-dimensional FE model of the structure (Figure 6b) has been developed by the research unit of the University of Perugia in the framework of previous research [67,89]. To provide more details, the authors reconstructed and calibrated a model using AVT data from May 2017. This model consisted of nine uniaxial high-sensitivity piezoelectric accelerometers, as documented in [89]. Initially, the model was separated into four parts: the Gattapone level (located beneath the square), the Arengo Hall level, the Nobili level (which includes the Campanari level), and the bell tower. To account for possible variations in material properties in these portions of the building, each part was assigned a distinct Young modulus value. Subsequently, in May 2021, a new AVT campaign was conducted (Section 3.1) by means of a dense sensor network (A1–A19 with reference to Figure 2). The model was then recalibrated, whereby the elastic modulus of nine predefined regions was adjusted (for further information, refer to [67]). These regions include the Arengo floor and the Gattapone level, the Nobili arched ceiling, the rooftop and its annexes, the loggia, the bell tower, the potential cracking patterns that can be activated by an earthquake evaluated as reported in [79] through nonlinear static analysis, the vertical walls along the x direction, and the vertical walls along the y direction.

Table 3 reports a general comparison between the two structural models in terms of number of nodes, elements, degrees of freedom (DOFs) resulting from the two discretizations, and the average elapsed time for the execution of different types of analysis (e.g., modal analysis (MA) and nonlinear static analysis (NLSA)) on a modern quad-core CPU. The difference in sophistication emerges immediately. The FE model has a number of DOFs three orders of magnitude greater than that of the EF companion. This huge increase in complexity grants the FE model unparalleled fidelity, at the cost of a dramatic increase in computational times—which are around 200 times longer for a modal analysis and in the order of ten thousand times longer for a nonlinear seismic analysis, such as NLSA.

**Table 3.** Comparison between the EF and FE models of the Consoli Palace.

	Equivalent Frame (EF)	Finite Element (FE)
Nodes	166 (2-D), 144 (3-D), 203 piers, 102 spandrels,	89 976 (3-D)
Elements	244 elastic beams, 15 4-nodes, and 95 3-nodes diaphragms	3 531 140 4-nodes tetrahedral solid elements
Free DOFs	969	3 418 097
Restrained DOFs	243	113 043
Total mass	28 383.666 ton	29 209.57 ton
Elapsed time for MA	≈4 s	≈1081.9 s
Elapsed time for NLSA	≈120 s	≈2.11 × 10 <sup>6</sup> s

Figure 7 summarizes the outcomes of the EF/FEM calibrations with respect to AVT experimental data, in terms of both mode shape correlation (MAC value) and relative difference  $\Delta f/f$  between numerical and experimental frequencies. In addition, a schematic depiction of the EF/FEM global mode shapes is illustrated. The EF calibration process (see Section 4.2), which is involving just four parameters, takes around 5 iterations (each with 4 parallel function evaluations to build the parameter sensitivity matrix) and 4 subiterations, for a total of 29 function evaluations completed in less than 1 min. Despite a rougher discretization, the EF model 7 is able to achieve a very good agreement with experimental identification, comparable with the results obtained by the FE model calibration. For both models, the percentage differences in frequency are lower than 4% for all the modes, and the MAC values always exceed 0.7. This result points out the possibility to reproduce the elastic behavior of the masonry palaces by means of a simplified EF formulation. It is important to emphasize that low values of the MAC indicator observed in the EF model for the local modes of the bell tower (modes L-F<sub>y</sub> and L-F<sub>x</sub>) are the result of updating choices. As explained later in the paper (Section 4.2), to ensure a robust continuous updating of the EF digital twin, the updating favors the optimization of frequency and mode shapes for the

global modes (those well captured by the permanent SHM system, which lacks sensors on the top of the bell tower), giving up some correlation for the local ones.

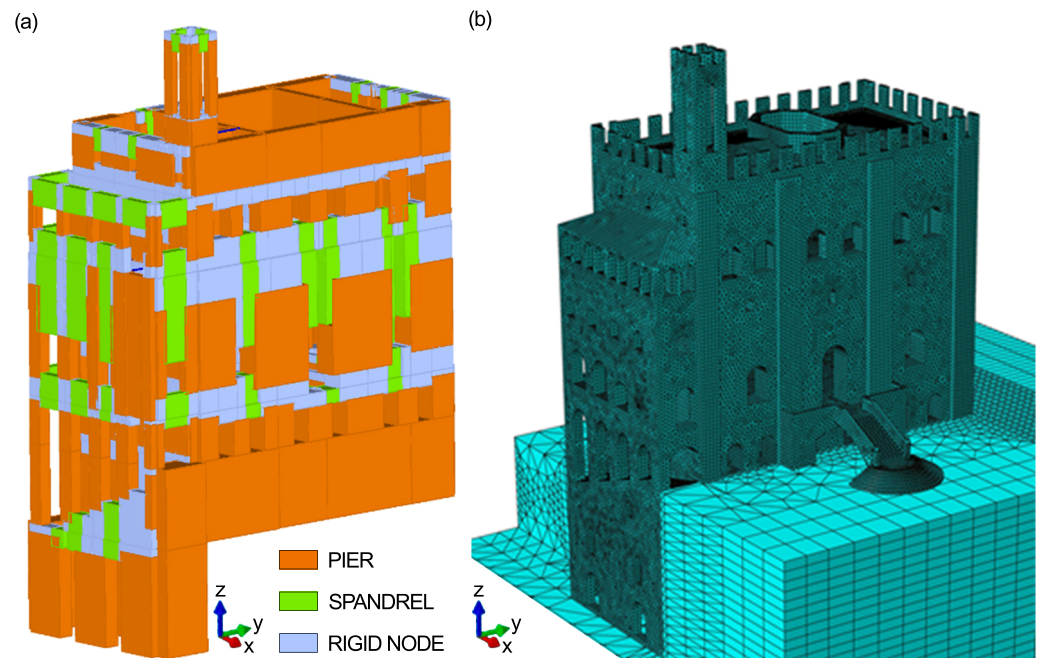


Figure 6. Structural models of the Consoli Palace: (a) EF model based on a structural element discretization and (b) high-fidelity FE model with a refined mesh.

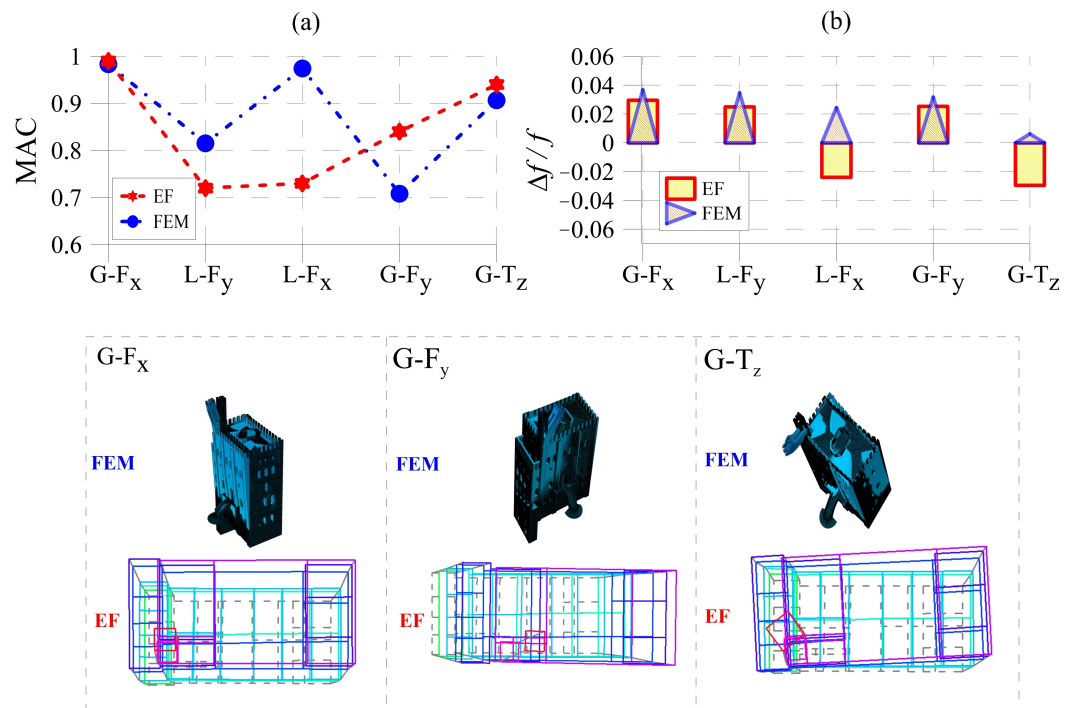


Figure 7. Comparison between FEM and EF calibration. (a) MAC values and (b) relative frequency difference  $\Delta f/f$ .

#### 4.2. EF Model Continuous Updating: Model-Driven Online Damage Assessment

In the following section, the EF structural model of the palace developed in Section 4.1 is combined, according to the proposal of Section 2.1, with the continuous flux of modal information identified from the dynamic monitoring system. The model is updated continuously based on daily-averaged identified natural frequencies and mode shapes, becoming a dynamically calibrated DT of the real structure. To give an exemplifying overview of the strengths and limitations of this strategy and, in particular, of its usefulness in the postseismic emergency, the updating procedure is carried out over a month of data, which includes the seismic sequence of 15 May 2021 (Section 3.2).

Thanks to its computational efficiency (see Table 3), the EF model of the structure is directly updated employing the well-known sensitivity method [53]. Out of the various techniques for updating structural models of engineering structures based on ambient vibration data [90] and for their optimization under different types of uncertainties [91], this approach has been one of the most successful and appears to be ideally suited for the framework of continuous model updating (in which, as discussed in Section 2.3, small perturbations are applied to the sensible parameters of the computational model which has been previously calibrated).

The optimization problem follows a weighted and regularized Levenberg–Marquardt scheme [92]

$$\left[ \mathbf{J}^T \mathbf{W} \mathbf{J} + \lambda \text{diag}(\mathbf{J}^T \mathbf{W} \mathbf{J}) \right] \delta = \mathbf{J}^T \mathbf{W} (\mathbf{y} - \hat{\mathbf{y}}(\mathbf{p})), \quad \mathbf{J} = \left[ \frac{\partial \hat{\mathbf{y}}(\mathbf{p})}{\partial \mathbf{p}} \right] \quad (1)$$

where  $\mathbf{y}$  and  $\hat{\mathbf{y}}$  are the target and model outputs,  $\mathbf{p}$  are the model parameters being updated,  $\mathbf{J}$  is the Jacobian matrix representing the local sensitivity of the model output  $\hat{\mathbf{y}}$  to variations in the parameters  $\mathbf{p}$ ,  $\mathbf{W}$  is a weighting matrix, and  $\lambda$  is the Levenberg–Marquardt damping parameter—steering the update between the Gauss–Newton (small  $\lambda$ ) and the gradient descent (large  $\lambda$ ) methods. Solving Equation (1) for  $\delta$  gives, at each iteration, the perturbation that minimizes the sum of the (weighted) squared errors, i.e., the function  $\chi^2$

$$\chi^2(\mathbf{p} + \delta) = \sum [\mathbf{y} - \hat{\mathbf{y}}(\mathbf{p} + \delta)]^2 \quad (2)$$

In accordance with the satisfying results previously obtained in the dynamic calibration of the EF model of the palace [88,93], only a few parameters are chosen for the continuous updating, in particular, those governing the stiffness of the palace and of the bell tower along each of the two main structural directions  $x$  and  $y$ . It is assumed that structural masses are quantified up to a satisfactory level of accuracy, whereas the elastic properties of the building material remain affected by a higher degree of uncertainty—no experimental test is available to characterize precisely the mechanical properties of masonry panels. Thus, the four sensible parameters undergoing the update are the Young moduli of the masonry of the palace walls directed along  $x$  and  $y$ ,  $E_{p,x}$  and  $E_{p,y}$  respectively, the same for the bell tower walls governed by the moduli  $E_{t,x}$  and  $E_{t,y}$ . These are the parameters to which the model's natural frequencies exhibit the most relevant sensitivity. The updating is carried out by normalizing all the moduli with respect to a reference value equal to  $p_{\text{ref}}$  equal to 4752 MPa, which is representative of a good-quality stone masonry.

Keeping the two directions independent from each other has a twofold objective, aimed at achieving a successful updating phase and a reliable damage localization. First, as discussed in [88], this expedient overcomes some limitations in the modeling of the out-of-plane stiffness of masonry elements in the assumed EF formulation, whose effect is significant due to the large thickness of the palace masonry walls. Second, from the point of view of structural analysis and seismic damage assessment, the choice of analyzing independently the two main directions is a common choice for masonry buildings—in which directional earthquake-resistant systems are easily identified from the architectonic configuration—allowing a more accurate interpretation of the response to earthquake actions and damage proneness of each resisting subsystem. Other uncertain parameters,

such as masonry mass density and the in-plane shear stiffness of vaults, are fixed according to the results obtained in previous calibrations (see [88]).

The Levenberg–Marquardt updating algorithm has been implemented in MATLAB (Mathworks, Inc., Natick, MA, USA, version R2023a) code, whereas TREMURI is handling the solution of the eigenvalue problems, for both the computation of the Jacobian sensitivity matrix  $\mathbf{J}$  by means of finite differences and the updating step. The target output  $\mathbf{y}$  is composed of the frequency of vibration of the first five modes and their mode shapes in all the locations sensed by the dynamic monitoring system (Section 3.2), excluding the out-of-plane measurements A11 and A12 (due to the absence of the corresponding degree-of-freedom in the EF model; see Section 4.1). The weighting matrix  $\mathbf{W}$  is assigning (i) a double relative weight to global modes with respect to local modes (given the absence of a dedicated SHM sensor at the top of the bell tower, Section 3.1) and (ii) the same relative weight to frequencies and mode shapes. The damping parameter  $\lambda$  is initialized to a value of  $1 \times 10^{-3}$  and updated according to [92]. Convergence is achieved if, at the end of a subiteration, the relative change in gradient or parameters  $\mathbf{p}$  is less than one part per cent or the relative change in the error function  $\chi^2$  is less than one part per thousand.

The results of the updating procedure are graphically summarized in Figure 8. The metrics used to evaluate the quality of the fit (the same employed first in Section 3.2 to assess damage from experimental measurements and later in Section 4.1 to compare the calibrated EF and FE models) are those typical of ambient vibration-based model updating procedures, i.e., (i) a global frequency-based metric aimed at parameter calibration, which is based on the relative difference in modal frequencies  $\Delta f/f$  and (ii) a spatial-based metric expressed through the MAC index, which ensures the one-to-one correspondence between experimental and numerical modes. The most interesting steps, in particular, the starting recalibration based on AVT, the first-day calibration on SHM data, and the updates across the day of the 15 May 2021 earthquake event, are reported in Tables 4 and 5 in terms of updated parameters (multiplicative coefficients  $cE_{p,x}$ ,  $cE_{p,y}$ ,  $cE_{t,x}$ ,  $cE_{t,y}$ ) and model output, respectively.

The starting recalibration based on AVT including the bell tower sensors (Section 3.1) is achieved in around four iterations and less than a minute of computation time (Table 4). The reasoning behind the overestimation of the Young modulus for the palace walls in the  $x$  direction with respect to those oriented in  $y$  (Table 5) can be traced back to the unmodeled out-of-plane stiffness, as pointed out in previous research from the authors [88].

Concerning SHM data, the model continuously reproduces the monitored behavior (Figure 8a), with relative frequency errors lower than 5% (Figure 8b) both before and after the day of the earthquake. The low-mode shapes correlation for local modes—MAC values around 0.7 for modes L- $F_y$  and L- $F_x$ ; Figure 8c—could be easily improved by increasing the mode shape weighting in the objective function, sacrificing some accordance in frequency. However, this choice is not suited for the purposes of this application, with mode shapes being typically less sensitive than frequencies to structural damage (as observed from experimental data; Section 3.2). It should be highlighted, moreover, that the local modes of the bell tower are governed by the atop modal amplification. The bell tower, even if explicitly modeled in the EF model, is not being directly monitored in the current setup of the SHM system (see Section 3.2).

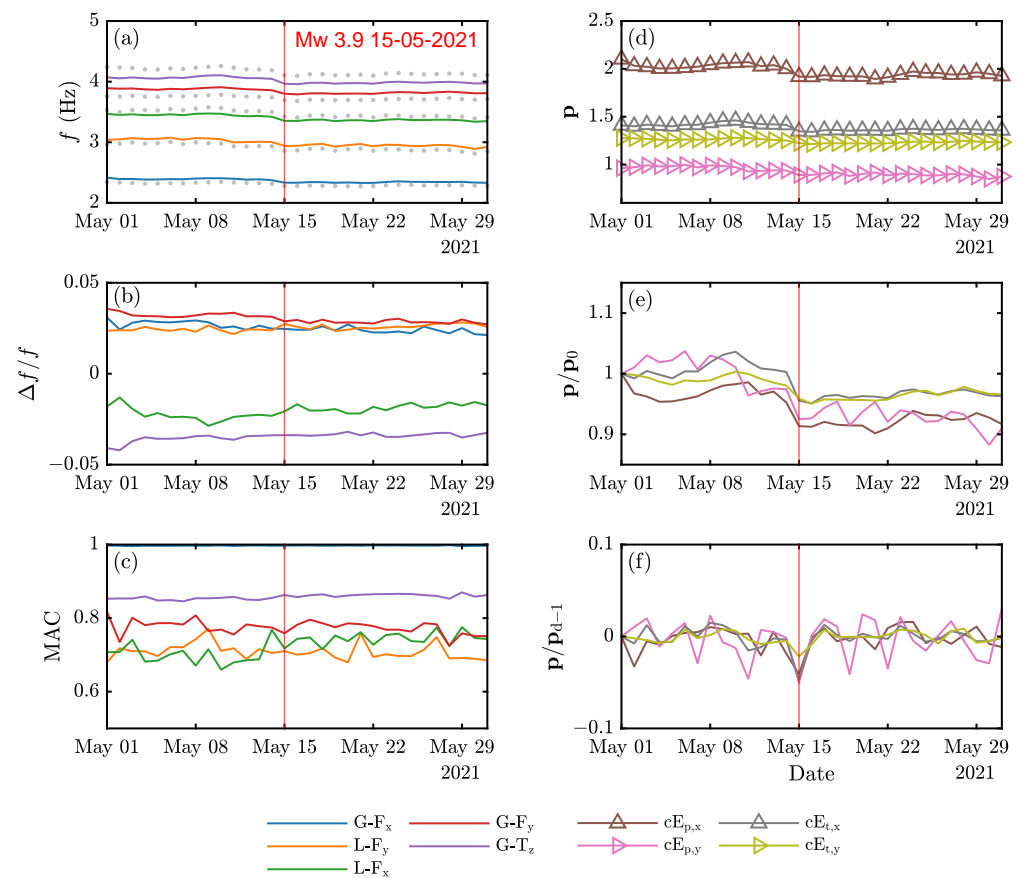


**Figure 8.** Results of the continuous updating of the EF model of the palace over the month of May 2021. (a) Model natural frequencies, (b) relative difference with respect to experimentally identified ones and (c) corresponding MAC, (d–f) values of the updated parameters  $\mathbf{p}$  and their relative variations with respect to the first calibration  $\mathbf{p}_0$  and previous-day calibration  $\mathbf{p}_{d-1}$ .

The behaviour over time of the updated parameters  $\mathbf{p}$  (Figure 8d) as well as the preliminary comparison with the first-day calibration  $\mathbf{p}_0$  highlight the permanent reduction of all the elastic moduli (Figure 8e). As shown by the comparison with the previous-day updating  $\mathbf{p}_{d-1}$ , such a reduction occurs on the day of the earthquake and with a different significance for each parameter (Figure 8f). Table 4 quantifies the relative change in the updated model parameters across the day of the earthquake, which are obtained with just two iterations and less than 20 s of computation, achieving a significant improvement of the error function  $\chi^2$ . The variations are clearly reductions—as expected from the lowering of the target frequencies due to structural damage; Section 3.2—and can be defined as mild in absolute terms, being always lower than 10%. In particular, the variations in the elastic moduli  $\mathbf{p}$  are estimated with respect to the reference value  $p_{ref}$ , to eliminate the influence of unmodeled out-of-plane stiffness from the damage assessment. The reduction across the day of the earthquake is much more significant along the x direction rather than y, affecting primarily the palace walls. This scenario is in agreement with the results of in-situ inspections, at least for what can be deduced from the evolution of pre-existing cracks [67], and shows a good overall agreement with the numerical results obtained from the Bayesian updating of the FE modal surrogate [79] (surrogate which is derived from the same calibrated FE model of the palace previously presented in Section 4.1).

**Table 4.** Updating of the EF model in the initial calibration (01-05-21) and for the days across the earthquake of 15 May 2021 (14-05-21 and 15-05-21). Values of the initial and updated multiplicative coefficient of the Young moduli of the palace masonry along each direction  $E_{p,x}$ ,  $E_{p,y}$  and the bell tower  $E_{t,x}$ ,  $E_{t,y}$ , value of the error function  $\chi^2$ , number of iterations and processing time.

Date	Initial p					Updated p					Iter.	Time (s)
	$cE_{p,x}$	$cE_{p,y}$	$cE_{t,x}$	$cE_{t,y}$	$\chi^2$	$cE_{p,x}$	$cE_{p,y}$	$cE_{t,x}$	$cE_{t,y}$	$\chi^2$		
May 2021 (AVT)	1	1	1	1	1.032	1.990	0.999	1.469	1.213	0.074	4	35.9
01-05-21 (SHM)	1.990	0.999	1.469	1.213	0.166	2.101	0.963	1.411	1.277	0.155	3	25.3
14-05-21	2.039	0.939	1.420	1.258	0.140	2.001	0.938	1.415	1.252	0.140	1	12.0
15-05-21	2.001	0.938	1.415	1.252	0.162	1.919	0.891	1.348	1.225	0.141	2	19.7
					$\Delta p/p_{ref}$	−0.082	−0.047	−0.067	−0.027			

A deeper understanding is obtained by looking at the average updated value of the parameters for the whole observation periods before and after the earthquake (Table 6), which should provide a more robust quantification of long-term permanent reductions. The scenario is quite similar to the one previously described, even though, for the palace walls, the differences between the two directions are less evident. This result could be related to an overfitting issue, which can be easily identified by looking at the lowering of the average error function  $\chi^2$  in the post-earthquake updating, if compared with the pre-event results. In particular, the model reaches a better fit with the frequency of the global mode G-F<sub>y</sub>, which could explain the significant decrease in the corresponding elastic moduli. Moreover, the fact that the identified frequency reductions following the 15 May earthquake are of the same order of magnitude as the average fitting error further complicates the analysis.

Nonetheless, for what concerns the bell tower, the updating procedure clearly suggests the x direction to be the most affected by seismic damage. This result seems to be in great accordance with the results of data-based damage localization, which highlighted the channel A2—at the rooftop level, in close proximity with the base of the bell tower and orientated along the x direction—as the location most affected by earthquake-induced damage (Section 3.2), confirming the reliability of the proposed model-driven assessment.

**Table 5.** Relative difference in frequency  $\Delta f/f$  and values of the MAC coefficient between the EF model and experimental data, for the initial calibration (01-05-21) and for the updating across the earthquake day of 15 May 2021 (14-05-21 and 15-05-21).

Mode	May 2021 (AVT)		01-05-21 (SHM)		14-05-21		15-05-21			
	Initial p	Updated p	Updated p	Updated p	Updated p	Updated p	Updated p			
	$\Delta f/f$	MAC	$\Delta f/f$	MAC	$\Delta f/f$	MAC	$\Delta f/f$	MAC		
G-F <sub>x</sub>	−0.177	0.961	0.029	0.990	0.0309	0.997	0.0248	0.997	0.0247	0.997
L-F <sub>y</sub>	−0.023	0.270	0.025	0.725	0.0237	0.680	0.0238	0.705	0.0274	0.710
L-F <sub>x</sub>	−0.156	0.563	−0.024	0.730	−0.0181	0.707	−0.0231	0.768	−0.0208	0.717
G-F <sub>y</sub>	−0.093	0.825	0.025	0.842	0.0357	0.817	0.0313	0.774	0.0288	0.759
G-T <sub>z</sub>	−0.163	0.481	−0.030	0.951	−0.0409	0.853	−0.0339	0.855	−0.0338	0.863

**Table 6.** Average value of the updated parameters  $\bar{\mathbf{p}}_{\text{pre}}$  and  $\bar{\mathbf{p}}_{\text{post}}$  referring to the pre- and post-earthquake updating, their relative change  $\Delta\bar{\mathbf{p}}/\mathbf{p}_{\text{ref}}$ . On the right side, a detailed comparison between model and target outputs.

	$\bar{\mathbf{p}}_{\text{pre}}$	$\bar{\mathbf{p}}_{\text{post}}$	$\Delta\bar{\mathbf{p}}/\mathbf{p}_{\text{ref}}$	Mode	$\bar{\chi}^2_{\text{pre}} = 0.149$		$\bar{\chi}^2_{\text{post}} = 0.136$	
					$\Delta\bar{f}/\bar{f}_{\text{pre}}$	$\overline{\text{MAC}}_{\text{pre}}$	$\Delta\bar{f}/\bar{f}_{\text{post}}$	$\overline{\text{MAC}}_{\text{post}}$
$cE_{p,x}$	2.036	1.935	−0.101	G- $F_x$	0.0273	0.997	0.0238	0.997
$cE_{p,y}$	0.968	0.893	−0.075	L- $F_y$	0.0241	0.715	0.0260	0.704
$cE_{t,x}$	1.423	1.361	−0.062	L- $F_x$	−0.0225	0.700	−0.0186	0.744
$cE_{t,y}$	1.266	1.230	−0.036	G- $F_y$	0.0324	0.780	0.0285	0.771
				G- $T_z$	−0.0360	0.853	−0.0335	0.862

#### 4.3. Offline Forecasting of the Postseismic Structural Behavior: An EF-Based Perspective

The computational models of the palace developed in Section 4.1, continuously fed by modal information provided by the dynamic monitoring system (Section 3.2) and updated to match experimental dynamics (Section 4.2), can be effectively employed as structural digital twins of the monitored structure.

The application presented in the following paragraphs should be intended as an exemplification of the proposal of Section 2.3. The EF model of the palace, updated in quasi real time based on vibration data acquired by the monitoring system and already employed online to obtain a quick estimation of the damage gravity (Section 4.2), is now employed in an offline environment to investigate the residual capacity of the building after the earthquake of 15 May 2021 (Section 3.2)—for example, in response to potential aftershocks.

Indeed, the reduction in frequencies experimentally identified on the structure (Section 3.2) is captured by the model updating procedure with respect to variations in the elastic parameters only—in this case, the elastic Young moduli of the masonry for different areas of the palace. It is plausible to assume that, in case of structural damage to the masonry panels, the resistance should be affected as well. As a first assumption, the relative reductions in masonry strength caused by seismic damage can be assumed to be equal to those identified for the elastic moduli by the updating procedure. This statement is supported by recent results of the literature, which investigated, through numerical simulations, the relationship between elastic and resistance parameters in masonry walls and its alteration due to aging and degradation effects [94]. The study results suggest that the respective reductions follow a linear trend with a regression coefficient very close to unity, thus validating the initial assumption.

Table 7 reports, on the left-hand side, the initial values of the parameters governing the strength of masonry panels. In particular, the maximum resistance corresponds to the minimum strength among the considered failure criteria—in this case, diagonal cracking for the shear failure according to the Turnšek and Čačovič criterion, rocking and crushing for the flexural one—and depends on the actual level of axial compression. The updating involves the peak compressive strength  $f_m$ , the peak tensile strength  $f_t$ , and the peak shear strength at zero confining stress  $f_{v0}$  (which is governing the equivalent tensile strength of spandrels [95]). As a dual approach to the update of the elastic Young moduli (Section 4.2), the strength parameters of the masonry are individually updated for each of the four areas of the palace previously considered. This implicitly assumes that areas with higher reductions of the elastic moduli, as identified from the optimization, are those more affected by structural damage with respect to not only their stiffness but also their strength. The updated parameters (subscript u) for each area—masonry walls of the palace body in the x and y directions, masonry walls of the bell tower in the x and y directions—are reported on the right-hand side of Table 7.

**Table 7.** Updated values (subscript u) of the masonry resistances, computed according to the results of the online updating (Section 4.2).

Area	Direction	$f_m$ (MPa)	$f_t$ (MPa)	$f_{v0}$ (MPa)	$1 + \Delta p/p$	$f_{m_u}$ (MPa)	$f_{t_u}$ (MPa)	$f_{v0_u}$ (MPa)
Palace	x				0.9180	3.6876	0.1279	0.2130
Palace	y	4.0170	0.1393	0.2320	0.9526	3.8266	0.1327	0.2210
Bell tower	x				0.9335	3.7497	0.1301	0.2166
Bell tower	y				0.9727	3.9074	0.1355	0.2257

By adopting a phenomenological constitutive model that describes the nonlinear response of masonry panels to monotonic and cyclic actions, implemented in the TREMURI research solver with the piecewise linear formulation proposed in [96], the EF model can simulate the nonlinear response of masonry panels until severe damage levels. This provides, in a time frame ranging from a few minutes for NLSA to a few hours for nonlinear dynamic analyses (NLDA) (in the last case, strongly depending on the global damage reached by the structure), a reliable forecast of the future global response of the building to potential aftershocks. In this application, NLSA is selected as the most suited approach to obtain a quick initial estimate of the residual capacity of the building after the earthquake of 15 May. For this purpose, a load pattern of horizontal forces proportional to floor masses is applied on the equivalent frame in the pre-earthquake—i.e., the calibrated model on the 14 May, representative of the reference undamaged state—and post-earthquake conditions—i.e., the calibrated model on the 15th of May, in which the reduced stiffnesses and resistances resulting from the updating procedure reproduce the damaged state caused by the earthquake.

Figure 9 shows a comparison between the pushover curves before and after the earthquake. The curves in the undamaged state exhibit (i) a ductile behavior in the x direction, i.e., along the shorter side, with a gradual drop of resistance starting at around 0.05 m of top displacement and a high displacement capacity, and (ii) a fragile behavior in the y direction, i.e., along the longer side, which is determined, despite the higher maximum resistance (a resistant shear around 50% higher than that of x), by the sudden and huge loss of resistant shear for top displacements of around 0.25 m, rapidly leading to higher damage states. The simulations carried out on the damaged model show a clear picture with respect to the loss of global stiffness. The stiffness reduction reproduces quite accurately the effects of the updating coefficients applied to the palace masonry moduli, with a reduction in the slope of the elastic part of the shear displacement curve equal to 7.1% and 5.0% in x and y direction, respectively. For what concerns resistance, along the y direction, i.e., the long side, only a negligible fraction of the maximum base reacting force, around 1.2%, is lost. On the other hand, the response of the building along the x direction appears to be more significantly affected, with a reduction of the maximum resistance of around 5.4% for forces applied in the positive verse.

Measurements of the palace's dynamic response to the earthquake are not available due to a power outage, which affected the monitoring system (Section 3.2). In this respect, the dynamic response to the earthquake simulated by NLDA on the calibrated EF model cannot be directly compared with experimental measurements. Nonetheless, this application can be extremely valuable to enhance the knowledge regarding damage diffusion and gravity acquired from data processing (Section 3.1) and model updating (Section 4.2). The calibrated EF model in the undamaged state (on 14 May) is thus subjected to the ground acceleration components measured by the close "Gubbio Parcheggio Santa Lucia" (GBSL) seismic station (see Section 3.2). In particular, given the proximity of the station, no attenuation law is applied to the signal. The horizontal components are suitably rotated in order to match the main directions of the palace, x and y, which form an angle with the north and east directions of around  $-30^\circ$  (see Figure 2).

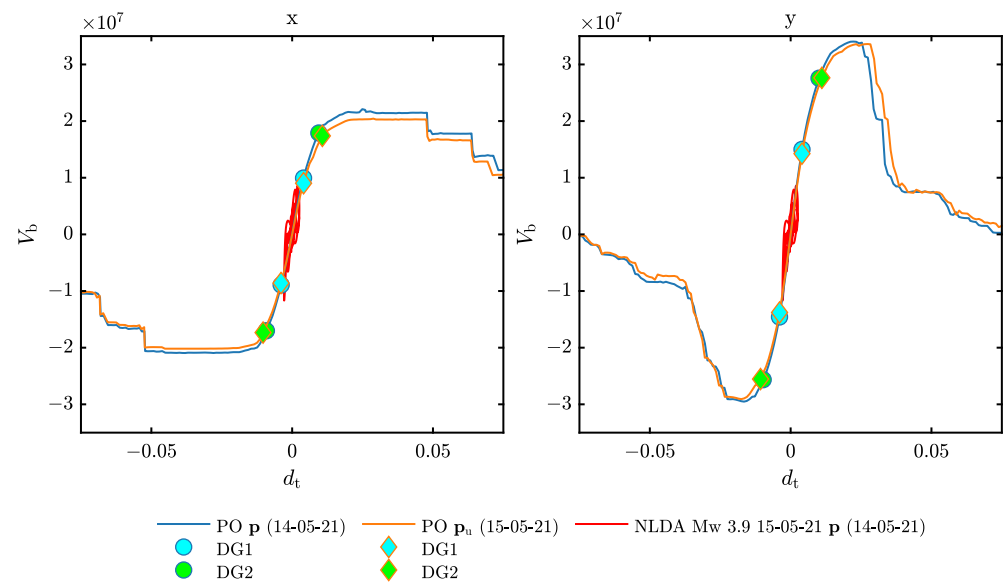


**Figure 9.** Comparison between pushover curves obtained from the continuously updated EF model in the pre-earthquake (14-05-21) and post-earthquake (15-05-21) conditions.

Figure 9 reports, in the base shear displacement plane, the response simulated through NLDA for the 15 May 2021 earthquake compared with that of NLSA. A first comparison with conventional damage thresholds on the pushover curve, respectively assumed for DG1 and DG2 as the attainment of 40% and 80% of the maximum strength in the increasing branch, suggests that the structure reached a global damage grade at least equal to DG1 for the x direction—defined as “negligible to slight damage (no structural damage, slight non-structural damage)” according to the EMS-98 scale. A more in-depth examination of the damage level (DL) reached by masonry walls, which is carried out according to the procedure proposed in [97], highlights how (i), globally, walls directed in the x direction exhibit more diffused damage than those in y but with low severity (Table 8) and (ii), regardless of the direction, a possible concentration of damage can be identified in the upper parts of the palace, at the Nobili level and in the bell tower (Figure 10). Both these results agree with the experimental evidence obtained from the processing of monitoring data and the in-situ inspections which pointed out x as the most affected direction and damage to be localized on the southern side of the palace, mainly in the upper floors (sensor A2; see Section 3.2). It can be concluded that, based on the DT-supported damage assessment, the palace has suffered negligible structural damages, mainly in the x direction, which does not undermine its seismic capacity. In this respect, the event did not increase significantly the building’s vulnerability to the possible occurrence of aftershocks.

**Table 8.** Percentage of walls that reached a certain DL for each direction.

Wall Damage Level	Self Weight		NLDA Mw 3.9 15-05-21	
	x (%)	y (%)	x (%)	y (%)
DL1	15.04	2.69	27.98	4.48
DL2	0	0.48	4.23	3.28
DL3	0	0	2.06	0.48
DL4	0	0	0	0

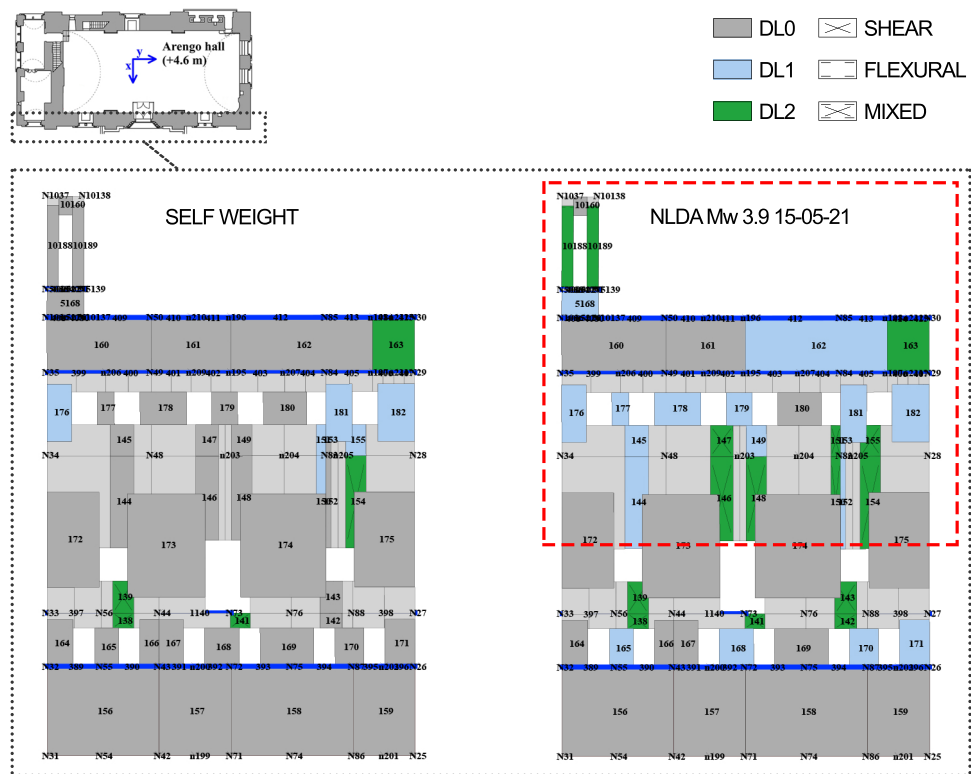


**Figure 10.** Results of NLDA on the EF model of the palace for the 15 May 2021 earthquake. The analysis is performed on the physics-enhanced DT, which is calibrated based on the previous-day modal identification (14-05-21). The model exhibits overall mild damage, which appears more diffused for the x direction (see Table 8). Nonetheless, some damage also occurs in the y direction, as shown in the figure for the facade, which suggests some damage concentration on the Nobili floor and in the bell tower.

## 5. Conclusions

The paper has proposed an innovative model-driven methodology, aimed at developing and continuously updating a physics-enhanced digital twin (DT) for the seismic health monitoring of historical masonry palaces. To illustrate the effectiveness of the proposed methodology, the Consoli Palace of Gubbio (Italy) is used as a compelling case study, a building continuously monitored by the authors since 2017.

A pivotal facet of the proposed methodology resides in the use of a computationally efficient physics-based representation of the monitored structure, the equivalent frame (EF) approach. Thanks to its computational lightness, the EF model of the palace is continuously calibrated based on modal properties identified from monitoring data, ensuring a heightened level of accuracy in capturing the structural behavior of the palace in operational and extreme conditions.

The study demonstrates the physics-based DT's prowess in unravelling the intrinsic physical phenomena and mechanisms governing the system behavior, enabling expeditious real-time localization and quantification of structural damage. By harnessing the dataset derived from a month of daily-identified modal properties in May 2021, the model's iterative enhancement process effectively showcased its prowess in discerning and localizing possible structural damages. The online updating procedure is able to closely reproduce the permanent decrease in natural frequencies identified after a minor seismic event on May 15th, quantifying the corresponding relative reductions in material stiffness from 3% to 8% of the pre-earthquake value for different parts of the building—with maximum reductions along the direction parallel to the short side of the building.

This capability is crucial for assessing the structural integrity of the palace after seismic events, allowing for quick responses in the post-earthquake decision making phase and providing valuable insights for long-term risk assessment and management. Moreover, through offline static and dynamic simulations of the nonlinear response performed after the earthquake, the physics-based DT is able to forecast in a short time frame the potential reduction in strength and capacity caused by seismic damage. Examining the preliminary online evaluations and the accurate offline analyses, it is possible to conclude that the investigated seismic event has not undermined the capacity of the building to resist future seismic actions.

The methodology developed in the paper constitutes a precious tool to support the seismic monitoring and risk assessment of historical masonry palaces, allowing for more effective risk management and preservation efforts and ultimately contributing to the sustainability of cultural heritage structures. The future sheds promising developments of the proposed approach, where the inherent reliance on physics-based principles allows for the application of prior knowledge. This feature enables the seamless adaptation of the model to diverse scenarios, system configurations and operating conditions, thereby enhancing its applicability and versatility.

**Author Contributions:** Conceptualization, D.S.; methodology, D.S. and S.C.; software, S.C.; formal analysis, D.S.; investigation, L.I.; writing—original draft preparation, D.S. and L.I.; writing—review and editing, S.C., F.U., and I.V.; visualization, D.S. and L.I.; supervision, S.C.; funding acquisition, S.C. and F.U. All authors have read and agreed to the published version of the manuscript.

**Funding:** This research was funded by the Italian Ministry of Education, University, and Research (MIUR) within the PRIN project DETECT-AGING “Degradation Effects on Structural Safety of Cultural Heritage constructions through simulation and health monitorING” (Call 2017—Protocol No. 201747Y73L).

**Data Availability Statement:** Not applicable.

**Acknowledgments:** The authors thankfully acknowledge the support of the PRIN project DETECT-AGING “Degradation Effects on Structural Safety of Cultural Heritage constructions through simulation and health monitorING” (Call 2017—Protocol No. 201747Y73L). The authors acknowledge aswell Sara Alfano for contributing to the development and preliminary calibration of the equivalent frame model of the palace.

**Conflicts of Interest:** The authors declare no conflict of interest.

## Abbreviations

The following abbreviations are used in this manuscript:

EF	equivalent frame
FE	finite element
DT	digital twin
CCLM	continuous constitutive law models
SEM	structural element models
SHM	structural health monitoring
S2HM	seismic structural health monitoring
SSI	stochastic subspace identification
MLR	multiple linear regression
PGA	peak ground acceleration
MAC	modal assurance criterion
COMAC	coordinate modal assurance criterion
DOF	degree of freedom
MA	modal analysis
NLSA	nonlinear static analysis
NLDA	nonlinear dynamic analysis
DG	damage grade (global scale)
DL	damage level (element scale)

## References

1. Avci, O.; Abdeljaber, O.; Kiranyaz, S.; Hussein, M.; Gabbouj, M.; Inman, D.J. A review of vibration-based damage detection in civil structures: From traditional methods to Machine Learning and Deep Learning applications. *Mech. Syst. Signal Process.* **2021**, *147*, 107077. [\[CrossRef\]](#)
2. Quqa, S.; Landi, L.; Diotallevi, P.P. Seismic structural health monitoring using the modal assurance distribution. *Earthq. Eng. Struct. Dyn.* **2021**, *50*, 2379–2397. [\[CrossRef\]](#)
3. Malekloo, A.; Ozer, E.; AlHamaydeh, M.; Girolami, M. Machine learning and structural health monitoring overview with emerging technology and high-dimensional data source highlights. *Struct. Health Monit.* **2022**, *21*, 1906–1955. [\[CrossRef\]](#)
4. Boje, C.; Guerriero, A.; Kubicki, S.; Rezgui, Y. Towards a semantic Construction Digital Twin: Directions for future research. *Autom. Constr.* **2020**, *114*, 103179. [\[CrossRef\]](#)
5. Jiang, F.; Ma, L.; Broyd, T.; Chen, K. Digital twin and its implementations in the civil engineering sector. *Autom. Constr.* **2021**, *130*, 103838. [\[CrossRef\]](#)
6. Callcut, M.; Cerceau Agliozzo, J.P.; Varga, L.; McMillan, L. Digital twins in civil infrastructure systems. *Sustainability* **2021**, *13*, 11549. [\[CrossRef\]](#)
7. Alanne, K.; Sierla, S. An overview of machine learning applications for smart buildings. *Sustain. Cities Soc.* **2022**, *76*, 103445. [\[CrossRef\]](#)
8. Bado, M.F.; Tonelli, D.; Poli, F.; Zonta, D.; Casas, J.R. Digital Twin for Civil Engineering Systems: An Exploratory Review for Distributed Sensing Updating. *Sensors* **2022**, *22*, 3168. [\[CrossRef\]](#)
9. Jouan, P.; Hallot, P. Digital twin: Research framework to support preventive conservation policies. *ISPRS Int. J. Geo-Inf.* **2020**, *9*, 228. [\[CrossRef\]](#)
10. Marra, A.; Trizio, I.; Fabbrocino, G. Digital Tools for the Knowledge and Safeguard of Historical Heritage. *Lect. Notes Civ. Eng.* **2021**, *156*, 645–662. [\[CrossRef\]](#)
11. Rainieri, C.; Rosati, I.; Cieri, L.; Fabbrocino, G. Development of the Digital Twin of a Historical Structure for SHM Purposes. *Lect. Notes Civ. Eng.* **2023**, *254*, 639–646. [\[CrossRef\]](#)
12. Wright, L.; Davidson, S. How to tell the difference between a model and a digital twin. *Adv. Model. Simul. Eng. Sci.* **2020**, *7*, 13. [\[CrossRef\]](#)
13. Degli Abbati, S.; Sivori, D.; Cattari, S.; Lagomarsino, S. Ambient vibrations-supported seismic assessment of the Saint Lawrence Cathedral's bell tower in Genoa, Italy. *J. Civ. Struct. Health Monit.* **2023**, 1–22. [\[CrossRef\]](#)
14. Angjeliu, G.; Coronelli, D.; Cardani, G. Development of the simulation model for Digital Twin applications in historical masonry buildings: The integration between numerical and experimental reality. *Comput. Struct.* **2020**, *238*, 106282. [\[CrossRef\]](#)
15. Funari, M.F.; Hajjat, A.E.; Masciotta, M.G.; Oliveira, D.V.; Lourenço, P.B. A parametric scan-to-FEM framework for the digital twin generation of historic masonry structures. *Sustainability* **2021**, *13*, 11088. [\[CrossRef\]](#)
16. Limongelli, M.P.; Çelebi, M. *Seismic Structural Health Monitoring: From Theory to Successful Applications*; Springer: Cham, Switzerland, 2019. [\[CrossRef\]](#)
17. Gattulli, V.; Franchi, F.; Graziosi, F.; Marotta, A.; Rinaldi, C.; Potenza, F.; Sabatino, U.D. Design and evaluation of 5G-based architecture supporting data-driven digital twins updating and matching in seismic monitoring. *Bull. Earthq. Eng.* **2022**, *20*, 4345–4365. [\[CrossRef\]](#)
18. Roca, P.; Cervera, M.; Gariup, G.; Pela', L. Structural analysis of masonry historical constructions. Classical and advanced approaches. *Arch. Comput. Methods Eng.* **2010**, *17*, 299–325. [\[CrossRef\]](#)
19. D'Altri, A.M.; Sarhosis, V.; Milani, G.; Rots, J.; Cattari, S.; Lagomarsino, S.; Sacco, E.; Tralli, A.; Castellazzi, G.; de Miranda, S. Modeling Strategies for the Computational Analysis of Unreinforced Masonry Structures: Review and Classification. *Arch. Comput. Methods Eng.* **2020**, *27*, 1153–1185. [\[CrossRef\]](#)
20. Lagomarsino, S.; Cattari, S. PERPETUATE guidelines for seismic performance-based assessment of cultural heritage masonry structures. *Bull. Earthq. Eng.* **2015**, *13*, 13–47. [\[CrossRef\]](#)
21. Cattari, S.; Calderoni, B.; Calìò, I.; Camata, G.; de Miranda, S.; Magenes, G.; Milani, G.; Satta, A. Nonlinear modeling of the seismic response of masonry structures: Critical review and open issues towards engineering practice. *Bull. Earthq. Eng.* **2022**, *20*, 1939–1997. [\[CrossRef\]](#)
22. Valente, M.; Milani, G. Non-linear dynamic and static analyses on eight historical masonry towers in the North-East of Italy. *Eng. Struct.* **2016**, *114*, 241–270. [\[CrossRef\]](#)
23. Betti, M.; Vignoli, A. Modelling and analysis of a Romanesque church under earthquake loading: Assessment of seismic resistance. *Eng. Struct.* **2008**, *30*, 352–367. [\[CrossRef\]](#)
24. Roca, P.; Cervera, M.; Pelà, L.; Clemente, R.; Chiumenti, M. Continuum FE models for the analysis of Mallorca Cathedral. *Eng. Struct.* **2013**, *46*, 653–670. [\[CrossRef\]](#)
25. Vila-Chã, E.; Barontini, A.; Lourenço, P.B. Implementation of a Condition Monitoring Strategy for the Monastery of Salzedas, Portugal: Challenges and Optimisation. *Buildings* **2023**, *13*, 719. [\[CrossRef\]](#)
26. Tiberti, S.; Acito, M.; Milani, G. Comprehensive FE numerical insight into Finale Emilia Castle behavior under 2012 Emilia Romagna seismic sequence: Damage causes and seismic vulnerability mitigation hypothesis. *Eng. Struct.* **2016**, *117*, 397–421. [\[CrossRef\]](#)

27. Degli Abbati, S.; D'Altri, A.M.; Ottonelli, D.; Castellazzi, G.; Cattari, S.; de Miranda, S.; Lagomarsino, S. Seismic assessment of interacting structural units in complex historic masonry constructions by nonlinear static analyses. *Comput. Struct.* **2019**, *213*, 51–71. [[CrossRef](#)]
28. Betti, M.; Galano, L. Seismic analysis of historic masonry buildings: The Vicarious Palace in Pescia (Italy). *Buildings* **2012**, *2*, 63–82. [[CrossRef](#)]
29. Clementi, F.; Pierdicca, A.; Formisano, A.; Catinari, F.; Lenci, S. Numerical model upgrading of a historical masonry building damaged during the 2016 Italian earthquakes: The case study of the Podestà palace in Montelupone (Italy). *J. Civ. Struct. Health Monit.* **2017**, *7*, 703–717. [[CrossRef](#)]
30. Valente, M. Seismic behavior and damage assessment of two historical fortified masonry palaces with corner towers. *Eng. Fail. Anal.* **2022**, *134*, 106003. [[CrossRef](#)]
31. Rolin, R.; Antaluca, E.; Batoz, J.L.; Lamarque, F.; Lejeune, M. From point cloud data to structural analysis through a geometrical hBIM-oriented model. *J. Comput. Cult. Herit.* **2019**, *12*, 1–26. [[CrossRef](#)]
32. Castellazzi, G.; Lo Presti, N.; D'Altri, A.M.; de Miranda, S. Cloud2FEM: A finite element mesh generator based on point clouds of existing/historical structures. *SoftwareX* **2022**, *18*, 101099. [[CrossRef](#)]
33. Lagomarsino, S.; Penna, A.; Galasco, A.; Cattari, S. TREMURI program: An equivalent frame model for the nonlinear seismic analysis of masonry buildings. *Eng. Struct.* **2013**, *56*, 1787–1799. [[CrossRef](#)]
34. Parisi, F.; Augenti, N. Seismic capacity of irregular unreinforced masonry walls with openings. *Earthq. Eng. Struct. Dyn.* **2013**, *42*, 101–121. [[CrossRef](#)]
35. Camata, G.; Marano, C.; Sepe, V.; Spacone, E.; Siano, R.; Petracca, M.; Roca, P.; Pelà, L. Validation of non-linear equivalent-frame models for irregular masonry walls. *Eng. Struct.* **2022**, *253*, 113755. [[CrossRef](#)]
36. Cattari, S.; D'Altri, A.M.; Camilletti, D.; Lagomarsino, S. Equivalent frame idealization of walls with irregular openings in masonry buildings. *Eng. Struct.* **2022**, *256*, 114055. [[CrossRef](#)]
37. Giongo, I.; Dizhur, D.; Tomasi, R.; Ingham, J.M. Field testing of flexible timber diaphragms in an existing vintage URM building. *J. Struct. Eng.* **2015**, *141*, D4014009. [[CrossRef](#)]
38. Sivori, D.; Lepidi, M.; Cattari, S. Structural identification of the dynamic behavior of floor diaphragms in existing buildings. *Smart Struct. Syst.* **2021**, *27*, 173–191. [[CrossRef](#)]
39. Cattari, S.; Resemini, S.; Lagomarsino, S. Modelling of vaults as equivalent diaphragms in 3D seismic analysis of masonry buildings. In Proceedings of the Structural Analysis of Historic Construction: Preserving Safety and Significance—Proceedings of the 6th International Conference on Structural Analysis of Historic Construction, SAHC08, Bath, UK, 2–4 July 2008; Volume 1, pp. 517–524.
40. Bianchini, N.; Mendes, N.; Calderini, C.; Candeias, P.; Rossi, M.; Lourenço, P. Seismic response of a small-scale masonry groin vault: Experimental investigation by performing quasi-static and shake table tests. *Bull. Earthq. Eng.* **2022**, *20*, 1739–1765. [[CrossRef](#)]
41. Lagomarsino, S.; Cattari, S.; Degli Abbati, S.; Ferrero, C. Valutazione della sicurezza statica e sismica del politeama “Giuseppe Verdi” a Carrara. In Proceedings of the IF CRASC 12, Pisa, Italy, 15–17 November 2012. (In Italian)
42. Rossi, M.; Cattari, S.; Lagomarsino, S. Performance-based assessment of the Great Mosque of Algiers. *Bull. Earthq. Eng.* **2015**, *13*, 369–388. [[CrossRef](#)]
43. Cattari, S.; Alfano, S.; Lagomarsino, S. A Practice-Oriented Proposal to Consider the Flange Effect in Equivalent Frame Modeling of Masonry Buildings. *Buildings* **2023**, *13*, 462. [[CrossRef](#)]
44. Cattari, S.; Degli Abbati, S.; Alfano, S.; Brunelli, A.; Lorenzoni, F.; da Porto, F. Dynamic calibration and seismic validation of numerical models of URM buildings through permanent monitoring data. *Earthq. Eng. Struct. Dyn.* **2021**, *50*, 2690–2711. [[CrossRef](#)]
45. Brunelli, A.; de Silva, F.; Piro, A.; Parisi, F.; Sica, S.; Silvestri, F.; Cattari, S. Numerical simulation of the seismic response and soil–structure interaction for a monitored masonry school building damaged by the 2016 Central Italy earthquake. *Bull. Earthq. Eng.* **2021**, *19*, 1181–1211. [[CrossRef](#)]
46. Degli Abbati, S.; Morandi, P.; Cattari, S.; Spacone, E. On the reliability of the equivalent frame models: The case study of the permanently monitored Pizzoli's town hall. *Bull. Earthq. Eng.* **2022**, *20*, 2187–2217. [[CrossRef](#)]
47. Mallardo, V.; Malvezzi, R.; Milani, E.; Milani, G. Seismic vulnerability of historical masonry buildings: A case study in Ferrara. *Eng. Struct.* **2008**, *30*, 2223–2241. [[CrossRef](#)]
48. Clementi, F.; Gazzani, V.; Poiani, M.; Lenci, S. Assessment of seismic behaviour of heritage masonry buildings using numerical modelling. *J. Build. Eng.* **2016**, *8*, 29–47. [[CrossRef](#)]
49. Malcata, M.; Ponte, M.; Tiberti, S.; Bento, R.; Milani, G. Failure analysis of a Portuguese cultural heritage masterpiece: Bonet building in Sintra. *Eng. Fail. Anal.* **2020**, *115*, 104636. [[CrossRef](#)]
50. Ponte, M.; Bento, R.; Vaz, S.D. A Multi-Disciplinary Approach to the Seismic Assessment of the National Palace of Sintra. *Int. J. Archit. Herit.* **2021**, *15*, 757–778. [[CrossRef](#)]
51. Lagomarsino, S.; Degli Abbati, S.; Ottonelli, D.; Cattari, S. Integration of modelling approaches for the seismic assessment of complex urm buildings: The podestà palace in Mantua, Italy. *Buildings* **2021**, *11*, 269. [[CrossRef](#)]
52. Jaishi, B.; Ren, W.X. Structural finite element model updating using ambient vibration test results. *J. Struct. Eng.* **2005**, *131*, 617–628. [[CrossRef](#)]

53. Mottershead, J.E.; Link, M.; Friswell, M.I. The sensitivity method in finite element model updating: A tutorial. *Mech. Syst. Signal Process.* **2011**, *25*, 2275–2296. [[CrossRef](#)]
54. Simoen, E.; De Roeck, G.; Lombaert, G. Dealing with uncertainty in model updating for damage assessment: A review. *Mech. Syst. Signal Process.* **2015**, *56*, 123–149. [[CrossRef](#)]
55. Marwala, T. *Finite-Element-Model Updating Using Computational Intelligence Techniques: Applications to Structural Dynamics*; Springer: London, UK, 2010; pp. 1–250. [[CrossRef](#)]
56. Bassoli, E.; Vincenzi, L.; D’Altri, A.M.; de Miranda, S.; Forghieri, M.; Castellazzi, G. Ambient vibration-based finite element model updating of an earthquake-damaged masonry tower. *Struct. Control. Health Monit.* **2018**, *25*, e2150. [[CrossRef](#)]
57. Bartoli, G.; Betti, M.; Marra, A.M.; Monchetti, S. A Bayesian model updating framework for robust seismic fragility analysis of non-isolated historic masonry towers. *Philos. Trans. R. Soc. A Math. Phys. Eng. Sci.* **2019**, *377*, 20190024. [[CrossRef](#)] [[PubMed](#)]
58. Pallarés, F.J.; Betti, M.; Bartoli, G.; Pallarés, L. Structural health monitoring (SHM) and Nondestructive testing (NDT) of slender masonry structures: A practical review. *Constr. Build. Mater.* **2021**, *297*, 123768. [[CrossRef](#)]
59. Ponsi, F.; Bassoli, E.; Vincenzi, L. Bayesian and deterministic surrogate-assisted approaches for model updating of historical masonry towers. *J. Civ. Struct. Health Monit.* **2022**, *12*, 1469–1492. [[CrossRef](#)]
60. Shabani, A.; Feyzabadi, M.; Kioumars, M. Model updating of a masonry tower based on operational modal analysis: The role of soil-structure interaction. *Case Stud. Constr. Mater.* **2022**, *16*, e00957. [[CrossRef](#)]
61. Cabboi, A.; Gentile, C.; Saisi, A. From continuous vibration monitoring to FEM-based damage assessment: Application on a stone-masonry tower. *Constr. Build. Mater.* **2017**, *156*, 252–265. [[CrossRef](#)]
62. Cavalagli, N.; Comanducci, G.; Ubertini, F. Earthquake-Induced Damage Detection in a Monumental Masonry Bell-Tower Using Long-Term Dynamic Monitoring Data. *J. Earthq. Eng.* **2018**, *22*, 96–119. [[CrossRef](#)]
63. Kita, A.; Cavalagli, N.; Venanzi, I.; Ubertini, F. On the use of digital twins for seismic structural health monitoring of a monumental masonry tower. In Proceedings of the 8th International Conference on Computational Methods in Structural Dynamics and Earthquake Engineering—COMPdyn 2021, Athens, Greece, 28–30 June 2021; pp. 346–353.
64. Kita, A.; Cavalagli, N.; Venanzi, I.; Ubertini, F. A new method for earthquake-induced damage identification in historic masonry towers combining OMA and IDA. *Bull. Earthq. Eng.* **2021**, *19*, 5307–5337. [[CrossRef](#)]
65. Pepi, C.; Gioffre’, M.; Grigoriu, M.D. Parameters identification of cable stayed footbridges using Bayesian inference. *Meccanica* **2019**, *54*, 1403–1419. [[CrossRef](#)]
66. García-Macías, E.; Ierimonti, L.; Venanzi, I.; Ubertini, F. An Innovative Methodology for Online Surrogate-Based Model Updating of Historic Buildings Using Monitoring Data. *Int. J. Archit. Herit.* **2021**, *15*, 92–112. [[CrossRef](#)]
67. Ierimonti, L.; Cavalagli, N.; Venanzi, I.; García-Macías, E.; Ubertini, F. A Bayesian-based inspection-monitoring data fusion approach for historical buildings and its post-earthquake application to a monumental masonry palace. *Bull. Earthq. Eng.* **2023**, *21*, 1139–1172. [[CrossRef](#)]
68. Penna, A.; Senaldi, I.E.; Galasco, A.; Magenes, G. Numerical Simulation of Shaking Table Tests on Full-Scale Stone Masonry Buildings. *Int. J. Archit. Herit.* **2016**, *10*, 146–163. [[CrossRef](#)]
69. Vanin, F.; Penna, A.; Beyer, K. Equivalent-Frame Modeling of Two Shaking Table Tests of Masonry Buildings Accounting for Their Out-Of-Plane Response. *Front. Built Environ.* **2020**, *6*. [[CrossRef](#)]
70. Tomić, I.; Vanin, F.; Božulić, I.; Beyer, K. Numerical simulation of unreinforced masonry buildings with timber diaphragms. *Buildings* **2021**, *11*, 205. [[CrossRef](#)]
71. Cattari, S.; Degli Abbati, S.; Ottonelli, D.; Marano, C.; Camata, G.; Spacone, E.; da Porto, F.; Modena, C.; Lorenzoni, F.; Magenes, G.; et al. Discussion on data recorded by the Italian structural seismic monitoring network on three masonry structures hit by the 2016–2017 Central Italy earthquake. In Proceedings of the 7th International Conference on Computational Methods in Structural Dynamics and Earthquake Engineering—COMPdyn 2019, Crete, Greece, 24–26 June 2019; pp. 1889–1906.
72. Martakis, P.; Reuland, Y.; Chatzi, E. Amplitude-dependent model updating of masonry buildings undergoing demolition. *Smart Struct. Syst.* **2021**, *27*, 157–172. [[CrossRef](#)]
73. Degli Abbati, S.; Cattari, S.; Lagomarsino, S. Validation of a practice-oriented floor spectra formulation through actual data from the 2016/2017 Central Italy earthquake. *Bull. Earthq. Eng.* **2022**, *20*, 7477–7511. . [[CrossRef](#)]
74. Sivori, D.; Cattari, S.; Lepidi, M. A methodological framework to relate the earthquake-induced frequency reduction to structural damage in masonry buildings. *Bull. Earthq. Eng.* **2022**, *20*, 4603–4638. [[CrossRef](#)]
75. MIT2018. Decreto Ministeriale del Ministero delle Infrastrutture e dei Trasporti del 17 Gennaio 2018. Aggiornamento delle «Norme Tecniche per le Costruzioni». Gazzetta Ufficiale Serie Generale n. 42 del 20/02/2018, Supplemento Ordinario n. 8. 2018. Available online: <https://www.gazzettaufficiale.it/eli/gu/2018/02/20/42/so/8/sg/pdf> (accessed on 10 March 2023). (In Italian)
76. Mirabella, F.; Ciaccio, M.; Barchi, M.; Merlini, S. The Gubbio normal fault (Central Italy): Geometry, displacement distribution and tectonic evolution. *J. Struct. Geol.* **2004**, *26*, 2233–2249. [[CrossRef](#)]
77. Chiaraluce, L.; Amato, A.; Carannante, S.; Castelli, V.; Cattaneo, M.; Cocco, M.; Collettini, C.; D’Alema, E.; Di Stefano, R.; Latorre, D.; et al. The alto Tiberina near fault observatory (northern Apennines, Italy). *Ann. Geophys.* **2014**, *57*. [[CrossRef](#)]
78. García-Macías, E.; Ubertini, F. MOVA/MOSS: Two integrated software solutions for comprehensive Structural Health Monitoring of structures. *Mech. Syst. Signal Process.* **2020**, *143*, 106830. . [[CrossRef](#)]

79. Ierimonti, L.; Venanzi, I.; García-Macías, E.; Ubertini, F. A transfer Bayesian learning methodology for structural health monitoring of monumental structures. *Eng. Struct.* **2021**, *247*, 113089. [[CrossRef](#)]
80. Gorini, A.; Nicoletti, M.; Marsan, P.; Bianconi, R.; De Nardis, R.; Filippi, L.; Marcucci, S.; Palma, F.; Zambonelli, E. The Italian strong motion network. *Bull. Earthq. Eng.* **2010**, *8*, 1075–1090. [[CrossRef](#)]
81. Pacor, F.; Paolucci, R.; Luzi, L.; Sabetta, F.; Spinelli, A.; Gorini, A.; Nicoletti, M.; Marcucci, S.; Filippi, L.; Dolce, M. Overview of the Italian strong motion database ITACA 1.0. *Bull. Earthq. Eng.* **2011**, *9*, 1723–1739. [[CrossRef](#)]
82. García-Macías, E.; Ubertini, F. Least Angle Regression for early-stage identification of earthquake-induced damage in a monumental masonry palace: Palazzo dei Consoli. *Eng. Struct.* **2022**, *259*, 114119. [[CrossRef](#)]
83. Allemang, R.J. The modal assurance criterion—Twenty years of use and abuse. *Sound Vib.* **2003**, *37*, 14–21.
84. Lieven, N.; Ewins, D. Spatial correlation of mode shapes, the coordinate modal assurance criterion (COMAC). In Proceedings of the 6th International Modal Analysis Conference—IMAC, Kissimmee, FL, USA, 1–4 February 1988; Volume 1, pp. 690–695.
85. Catbas, F.; Aktan, A.; Allemang, R.; Brown, D. Correlation function for spatial locations of scaled mode shapes—(COMEF). In Proceedings of the 16th International Modal Analysis Conference—IMAC, Santa Barbara, CA, USA, 2–5 February 1998; Volume 2, pp. 1550–1555.
86. Hunt, D.L. Application of an enhanced coordinate modal assurance criterion. In Proceedings of the 10th International Modal Analysis Conference—IMAC, San Diego, CA, USA, 3–7 February 1992; Volume 1, pp. 66–71.
87. Brughmans, M.; Leuridan, J.; Blauwkamp, K. The application of FEM-EMA correlation and validation techniques on a body-in-white. In Proceedings of the Measurement Science Conference—MSC, Anaheim, CA, USA, May 1993; p. 646.
88. Cattari, S.; Sivori, D.; Alfano, S.; Ierimonti, L.; Cavalagli, N.; Venanzi, I.; Ubertini, F. Calibration of numerical models to support SHM: The consoli palace of Gubbio, Italy. In Proceedings of the 8th International Conference on Computational Methods in Structural Dynamics and Earthquake Engineering—COMPdyn 2021, Athens, Greece, 28–30 June 2021; pp. 3778–3794.
89. Kita, A.; Cavalagli, N.; Ubertini, F. Temperature effects on static and dynamic behavior of Consoli Palace in Gubbio, Italy. *Mech. Syst. Signal Process.* **2019**, *120*, 180–202. [[CrossRef](#)]
90. Girardi, M.; Padovani, C.; Pellegrini, D.; Robol, L. A finite element model updating method based on global optimization. *Mech. Syst. Signal Process.* **2021**, *152*, 107372. [[CrossRef](#)]
91. Yang, C.; Yu, Q. Placement and size-oriented heat dissipation optimization for antenna module in space solar power satellite based on interval dimension-wise method. *Aerosp. Sci. Technol.* **2023**, *134*, 108155. [[CrossRef](#)]
92. Marquardt, D.W. An algorithm for least-squares estimation of nonlinear parameters. *J. Soc. Ind. Appl. Math.* **1963**, *11*, 431–441. [[CrossRef](#)]
93. Sivori, D.; Alfano, S.; Cattari, S.; Ierimonti, L.; Venanzi, I.; Ubertini, F. Nonlinear static analyses to improve the seismic damage assessment of monitored masonry palaces: Application to the Consoli Palace of Gubbio, Italy. XIX ANIDIS Conference, Seismic Engineering in Italy. *Procedia Struct. Integr.* **2023**, *44*, 2090–2097. [[CrossRef](#)]
94. Saviano, F.; Parisi, F.; Lignola, G.P. Material aging effects on the in-plane lateral capacity of tuff stone masonry walls: A numerical investigation. *Mater. Struct. Constr.* **2022**, *55*, 198. [[CrossRef](#)]
95. Cattari, S.; Lagomarsino, S. A strength criterion for the flexural behaviour of spandrels in un-reinforced masonry walls. In Proceedings of the 14th World Conference on Earthquake Engineering—14WCEE, Beijing, China, 12–17 October 2008.
96. Lagomarsino, S.; Cattari, S. Seismic Performance of Historical Masonry Structures through Pushover and Nonlinear Dynamic Analyses. In *Perspectives on European Earthquake Engineering and Seismology*; Ansal, A., Ed.; Springer International Publishing: Cham, Switzerland, 2015; Volume 2, pp. 265–292. [[CrossRef](#)]
97. Cattari, S.; Angiolilli, M. Multiscale procedure to assign structural damage levels in masonry buildings from observed or numerically simulated seismic performance. *Bull. Earthq. Eng.* **2022**, *20*, 7561–7607. [[CrossRef](#)]

**Disclaimer/Publisher’s Note:** The statements, opinions and data contained in all publications are solely those of the individual author(s) and contributor(s) and not of MDPI and/or the editor(s). MDPI and/or the editor(s) disclaim responsibility for any injury to people or property resulting from any ideas, methods, instructions or products referred to in the content.